

Generation of *N*-Methyl-D-aspartate Agonist and Competitive Antagonist Pharmacophore Models. Design and Synthesis of Phosphonoalkyl-Substituted Tetrahydroisoquinolines as Novel Antagonists

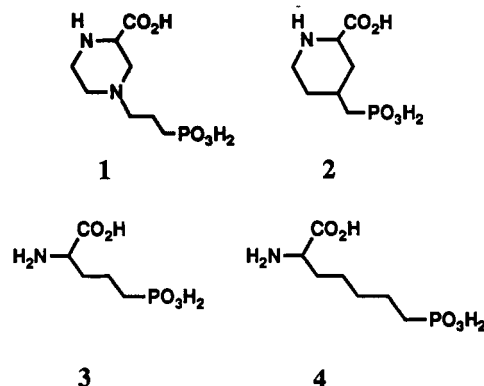
Daniel F. Ortwine,*[†] Thomas C. Malone,* Christopher F. Bigge, James T. Drummond, Christine Humblet, Graham Johnson, and Garry W. Pinter

Department of Chemistry, Parke-Davis Pharmaceutical Research Division, Warner-Lambert Company, 2800 Plymouth Road, Ann Arbor, Michigan 48105. Received March 13, 1991

The preparation and binding affinity of a series of tetrahydroisoquinoline carboxylic acids at the *N*-methyl-D-aspartate (NMDA) subtype of the glutamate receptor is described, together with a molecular modeling analysis of NMDA agonists and antagonists. Using published NMDA ligands, the active analogue mapping approach was employed in the generation of an agonist pharmacophore model. Although known competitive antagonists such as CPP (1) could be superimposed onto the agonist model, to overcome the assumption that they bind to the same receptor site, an independent modeling approach was used to derive a separate pharmacophore model. Development of a competitive antagonist model involved a stepwise approach that included the definition of a preferred geometry for PO₃H₂-receptor interactions, multiple conformational searches, and the determination of volume and electronic tolerances. This model, which is described in detail, is consistent with observed affinities of potent NMDA antagonists and has provided an explanation for the observed periodicity in affinities for the known antagonists AP5, AP6, and AP7. The features of the agonist and antagonist models are compared, and hypotheses advanced about the nature of the receptor interactions for these two classes of compounds. The pharmacophore models reported herein are consistent with a single recognition site at the NMDA receptor that can accommodate both agonist and antagonist ligands. To assist in first defining and later exploring the predictive power of the competitive antagonist model, a series of conformationally constrained NMDA antagonist (phosphonoalkyl)tetrahydroisoquinoline-1- and 3-carboxylates was prepared. From this work, 1,2,3,4-tetrahydro-5-(2-phosphonoethyl)-3-isoquinolinecarboxylic acid (89) was identified as the most active lead structure, with an IC₅₀ of 270 nM in [³H]CPP binding. The synthesis and structure-activity relationships of these novel antagonists are described.

Receptors for the excitatory amino acids glutamate and aspartate have been implicated in the pathology of a number of neurological and neurodegenerative disorders. These include epilepsy and spasticity, stroke, Huntington's and Alzheimer's diseases, and more recently, schizophrenia.¹ Several receptor subtypes have now been characterized, including those specific for *N*-methyl-D-aspartic acid (NMDA), α -amino-3-hydroxy-5-methyl-4-isoxazolepropanoic acid (AMPA), kainic acid (KA), 2-amino-3-phosphonopropanoic acid (AP4), and 1-amino-1,3-cyclopentanedicarboxylic acid (ACPD) (a G-protein coupled glutamic acid receptor).²

Although the NMDA-receptor subtype has been particularly well studied, it is not clear how agonists and competitive antagonists interact at the glutamate recognition site. Isolation of possible protein subunits has provided clues to the overall structural composition of the NMDA receptor complex.^{3,4} However, this complex has not yet been expressed and thus the three-dimensional organization of atoms in the receptor site is unknown. Instead, medicinal and computational chemistry techniques, through new, potent ligands, have afforded some insight into receptor structure. Thus, examination of the SAR and conformational properties of NMDA agonists⁵ and antagonists⁶ has led to the generation of agonist-preferring "pseudoreceptor"⁷ and schematic antagonist^{6b,8} receptor models. Although competitive antagonists such as CPP (1), CGS 19755 (2), AP5 (3), and AP7 (4) are potent *in vitro*, they are conformationally flexible and suffer from poor CNS bioavailability, presumably due to their polar, hydrophilic nature.^{9,10} Knowledge of the biologically significant conformation, together with areas of the structure that are amenable to variation (bulk tolerance), would permit the design of antagonists with increased rigidity and lipophilicity, and therefore hopefully potency and selectivity.



Previously, the synthesis and NMDA-receptor affinity of a series of AP7 analogues containing a phenyl spacer that reduced conformational flexibility were reported.¹¹ In the current study, two series of tetrahydroisoquinoline derivatives were synthesized in an attempt to further restrict conformational degrees of freedom while maintaining

- (1) (a) Wachtel, H.; Turski, L.; Glutamate: A New Target in Schizophrenia? *Trends Pharmacol. Sci.* 1990, 11, 219-220. (b) Olney, J. W. Excitotoxic Amino Acids and Neuropsychiatric Disorders. *Annu. Rev. Pharmacol. Toxicol.* 1990, 30, 47-71. (c) Meldrum, B. Protection Against Ischaemic Neuronal Damage by Drugs Acting on Excitatory Neurotransmission. *Cerebrovasc. Brain Metab. Rev.* 1990, 2, 27-57. (d) Albers, G. W. Potential Therapeutic Uses of *N*-methyl-D-aspartate Antagonists in Cerebral Ischemia. *Clin. Neuropharmacol.* 1990, 13, 177-197. (e) Carlsson, M.; Carlsson, A. Interactions Between Glutamatergic and Monoaminergic Systems within the Basal Ganglia-Implications for Schizophrenia and Parkinson's Disease. *Trends Neuro. Sci.* 1990, 13, 272-276. (f) Kornhuber, J. Glutamate and Schizophrenia [letter]. *Trends Pharmacol. Sci.* 1990, 11, 357. (g) Choi, D. W.; Rothman, S. M. The Role of Glutamate Neurotoxicity in Hypoxic-Ischemic Neuronal Death. *Annu. Rev. Neurosci.* 1990, 13, 171-182. (h) Meldrum, B. S.; Garthwaite, J. Excitatory Amino Acid Neurotoxicity and Neurodegenerative Disease. *Trends Pharmacol. Sci.* 1990, 11, 379-387.

[†]To whom correspondence on molecular modeling should be addressed.

affinity for the NMDA receptor.¹² These compounds, together with the recent reports of relatively rigid, potent, and selective NMDA-receptor ligands,^{6b,13} have facilitated the use of the active analogue pharmacophore mapping approach¹⁴ in the generation of predictive agonist and competitive antagonist pharmacophore models. Therefore, in parallel with the synthesis, molecular modeling studies of NMDA agonists and competitive antagonists were undertaken, incorporating newly synthesized isoquinolines as well as other recently reported analogues as they became available.

This communication describes the derivation of these models, their major characteristics and the differences between them, and their use in the design of second-generation phosphonoalkyl-substituted isoquinolines. The rationale behind the preparation of an initial set of isoquinolines as well as the synthesis and SAR of the entire set of isoquinolines is also presented.

Molecular Modeling

Overall Strategy. At the outset of the modeling analyses, few reports on competitive NMDA antagonists other than compounds 1-4 had appeared in the literature. However, the receptor affinities of a number of agonists had been described.

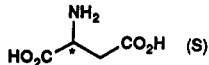
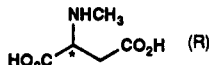
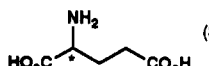
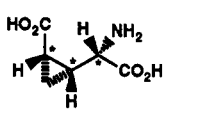
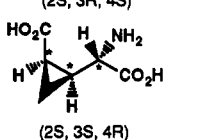
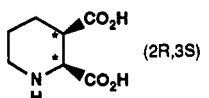
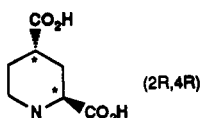
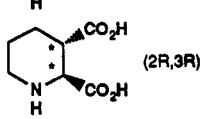
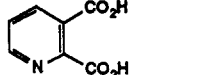
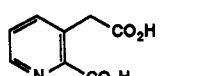
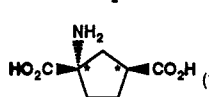
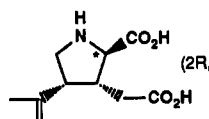
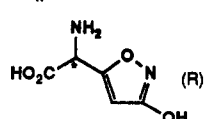
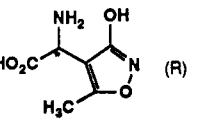
Therefore, as a stepping stone toward an understanding of how the larger, more flexible antagonists might interact

at the NMDA receptor, we undertook a study of the smaller, relatively rigid agonists that were reported in the literature at the time. It was our intent to gain a basic, qualitative feel of if the agonists could, in a reasonably low energy conformation, be made to interact in a common fashion within a hypothetical receptor site. To this end, an initial set of NMDA agonists selected from literature data were used to elaborate a qualitative agonist pharmacophore model (see the agonist modeling section below).

Although known competitive antagonists such as CPP (1) could be superimposed onto the initial agonist model under the assumption of a similar binding mode, the increased structural variety encountered in antagonist analogues that were synthesized in our laboratories or reported in the literature during the course of the analysis of agonists prompted an independent modeling approach toward the description of a separate pharmacophore model. The development of a competitive antagonist model involved a stepwise approach that included the definition of a preferred geometry for PO₃H₂-receptor interactions, multiple conformational searches, and the determination of volume and electronic requirements. The features of the initial agonist and antagonist models were then compared, and hypotheses were generated about the nature

- (2) For recent reviews, see: (a) Watkins, J. C.; Krosggaard-Larsen, P.; Honore, T. Structure-Activity Relationships in the Development of Excitatory Amino Acid Receptor Agonists and Competitive Antagonists. *Trends Pharmacol. Sci.* **1990**, *11*, 25-33. (b) Hansen, J. J.; Krosggaard-Larsen, P. Structural, Conformational, and Stereochemical Requirements of Central Excitatory Amino Acid Receptors. *Med. Res. Rev.* **1990**, *10*, 55-94. (c) *The NMDA Receptor*; Watkins, J. C., Collingridge, G. L., Eds.; Oxford University Press: Oxford, 1989.
- (3) (a) Ikin, A. F.; Kloog, Y.; Sokolovsky, M. N-methyl-D-aspartate/phencyclidine Receptor Complex of Rat Forebrain: Purification and Biochemical Characterization. *Biochemistry* **1990**, *29*, 2290-2295. (b) Eaton, M. J.; Chen, J.-W.; Kumar, K. N.; Cong, Y.; Michaelis, E. K. Immunochemical Characterization of Brain Synaptic Membrane Glutamate-Binding Proteins. *J. Biol. Chem.* **1990**, *265*, 16195-16204.
- (4) Cunningham, M. D.; Michaelis, E. K. Solubilization and Partial Purification of 3-(+)-2-carboxypiperazine-4-yl-[1,2-³H]propyl-1-phosphonic Acid Recognition Proteins from Rat Brain Synaptic Membranes. *J. Biol. Chem.* **1990**, *265*, 7768-7778.
- (5) (a) Madsen, U.; Brehm, L.; Schaumberg, K.; Jorgensen, F. S.; Krosggaard-Larsen, P. Relationship Between Structure, Conformational Flexibility, and Biological Activity of Agonists and Antagonists at the N-methyl-D-aspartic Acid Subtype of Excitatory Amino Acid Receptors. *J. Med. Chem.* **1990**, *33*, 374-380. (b) Nielson, E. O.; Madsen, U.; Schaumberg, K.; Brehm, L.; Krosggaard-Larsen, P. Studies on Receptor-Active Conformations of Excitatory Amino Acid Agonists and Antagonists. *Eur. J. Med. Chem.* **1986**, *21*, 433-437. (c) Davies, J.; Evans, R. H.; Francis, A. A.; Jones, A. W.; Smith, D. A.; Watkins, J. C. Conformational Aspects of the Actions of Some Piperidine Dicarboxylic Acids at Excitatory Amino Acid Receptors in the Mammalian and Amphibian Spinal Cord. *Neurochem. Res.* **1982**, *7*, 1119-1133.
- (6) (a) Olverman, A. W.; Jones, A. W.; Mewett, K. N.; Watkins, J. C. Structure/activity Relations of N-methyl-D-aspartate Receptor Ligands as Studied by their Inhibition of [³H]D-2-amino-5-phosphonopentanoic Acid Binding in Rat Brain Membranes. *Neuroscience* **1988**, *26*, 17-31. (b) Hutchinson, A. J.; Williams, A.; Angst, C.; de Jesus, R.; Blanchard, L.; Jackson, R. H.; Wilusz, E. J.; Murphy, D. E.; Bernard, P. S.; Schneider, J.; Campbell, T.; Guida, W.; Sills, M. A. 4-(Phosphonoalkyl)- and 4-(phosphonoalkenyl)-2-piperidinecarboxylic acids: Synthesis, Activity at N-methyl-D-aspartic Acid Receptors, and Anticonvulsant Activity. *J. Med. Chem.* **1989**, *32*, 2171-2178.
- (7) (a) Rao, S. N.; Snyder, J. P. Pseudoreceptor modeling. An experiment in large-scale computing. *Cray Channels* **1990**, winter issue, 8. (b) Snyder, J. P.; Rao, S. N.; Pellicciari, R.; Monahan, J. B. Receptor modeling of highly charged excitatory amino acids using the molecular dynamics/free energy perturbation approach. In *Frontiers in Drug Research*, Alfred Benzon Symposium 28; Jensen, B., Jorgensen, F. S., Kofod, H., Eds.; Munksgaard: Copenhagen, 1990; pp 109-118.
- (8) (a) Watkins, J. C. In *Fast and Slow Signalling in the Nervous System*; Iverson, L. L., Goodman, E. G., Eds.; Oxford University Press: Oxford, 1986; pp 89-105. (b) Fagg, G. E.; Baud, J. Characterization of NMDA Receptor-Ionophore Complexes in the Brain. In *Excitatory Amino Acids in Health and Disease*; Lodge, D., Ed.; John Wiley & Sons, Ltd., 1988; pp 63-90.
- (9) The measured log of P of 1 is -3.4. See ref 10a.
- (10) (a) Hays, S. J.; Bigge, C. F.; Novak, P. M.; Drummond, J. T.; Bobovski, T. P.; Rice, M. J.; Johnson, G.; Brahce, L. J.; Coughenour, L. L. New and Versatile Approaches to the Synthesis of CPP-related Competitive NMDA Antagonists. Preliminary Structure-Activity Relationships and Pharmacological Evaluation. *J. Med. Chem.* **1990**, *33*, 2916-2924. (b) The level of radioactivity in the brain of [³H]AP7 (4) corresponded to approximately 0.1% of the total amount of tritium injected. Compton, R. P.; Hood, W. F.; Monahan, J. B. Determination of the Pharmacokinetics of 2-amino-7-phosphonoheptanoate in Rat Plasma and Cerebrospinal Fluid. *Neurosci. Lett.* **1988**, *84*, 339-344. (c) Chapman, A. G.; Collins, J. F.; Meldrum, B. S.; Westerburg, E. Uptake of a Novel Anticonvulsant Compound, 2-amino-7-phosphono-[4,5-³H]heptanoic acid, into Mouse Brain. *Neurosci. Lett.* **1983**, *37*, 75-80.
- (11) Bigge, C. F.; Drummond, J. T.; Johnson, G.; Malone, T.; Probert, A. W., Jr.; Marcoux, F. W.; Coughenour, L. L.; Brahce, L. J. Exploration of Phenyl-spaced 2-Amino-(5-9)-phosphonoalkanoic Acids as Competitive N-methyl-D-aspartic acid Antagonists. *J. Med. Chem.* **1989**, *32*, 1580-1590.
- (12) While this manuscript was in preparation the synthesis of compounds 87 and 88 was reported; see: Cordi, A.; Vazquez, M. L. European Patent Application 364,996, 1990.
- (13) Pellicciari, R.; Natalini, B.; Marinozzi, M.; Selvi, L.; Chiorri, C.; Monahan, J. B.; Lanthorn, T. H.; Snyder, J. P. 3,4-Cyclopropyl Glutamates As Conformationally Restricted Agonists of the NMDA Receptor. In *Frontiers in Excitatory Amino Acid Research*; Cavalheiro, E. A., Lehmann, J., Turski, L., Eds.; Alan R. Liss, Inc.: New York, 1988; pp 67-70.
- (14) Marshall, G. R.; Barry, C. D.; Bosshard, H. E.; Dammkoehler, R. A.; Dunn, D. A. The Conformational Parameter in Drug Design: The Active Analog Approach. *Computer-Assisted Drug Design*; Olson, E. C., Christofferson, R. E., Eds.; ACS Symposium Series 112; American Chemical Society: Washington, DC, 1979; pp 205-226.

Table I. NMDA Agonists Used To Describe the Pharmacophore Model

no.	name	ref(s)	relative affinity ^a	structure ^b	energies, kcal/mol				
					RMS ^c	spring ^d	total ^e	relaxed ^f	cost ^g
5	L-ASP	42	++	 (S)	0.2	3.9	5.8	-0.8	2.7
6	NMDA	43	++	 (R)	0.05	0.4	1.3	-0.2	1.1
7	L-GLU	43	+++	 (S)	0.2 0.4 ^h	3.6	13.2	1.8	7.8
8	D-CGA-C	12	++++	 (2S, 3R, 4S)	0.2	3.0	104.2	98.8	2.4
9	D-CGA-D	12	++	 (2S, 3S, 4R)	0.2	4.6	108.0	100.4	3.0
10	PDA	43-46	+	 (2R,3S)	0.04	0.2	-1.4	-2.4	0.8
11	PDA	43-46	+	 (2R,4R)	0.2	3.3	3.9	-2.4	2.9
12	PDA	43-46	++	 (2R,3R)	0.1	2.0	7.1	2.5	2.6
13	QUIN	8b	+		0.08	0.9	6.2	3.9	1.3
14	HOMOQUIN	8b	++		0.1	0.8	2.6	1.0	0.9
15	ACPD	43, 47	++	 (1R, 3R)	0.2	2.9	7.4	2.4	2.1
16	D-KA	43	+	 (2R, 3R, 4R)	0.2 0.5 ^h	6.0	14.6	4.5	4.0
17	D-IBO	43	++	 (R)	0.3 0.4 ^h	10.2	24.5	7.8	6.5
18	D-AMAA	48, 49	++	 (R)	0.2 0.4 ^h	6.5	20.5	7.3	6.7

^a For displacement of [³H]Glu or [³H]AP5, generally from rat brain membranes. Because different radioligands were used by different laboratories in testing, only categorical data are presented. The categories were defined as follows: (++++), $K_i < 0.1 \mu\text{M}$; (+++), K_i between 0.1 and 1.0 μM ; (++) , K_i between 1 and 10 μM ; and (+), K_i between 10 and 1000 μM . ^b Stars on the structures denote chiral atoms. The stereoisomer employed in the analysis is given next to the structure in parentheses. ^c Deviation, in angstroms, between atoms employed in the fitting process. These deviations are relative to the average positions of the fitting atoms as determined using the entire set of agonists. Higher values reflect a less precise fit. ^d Spring energy between fit atoms. Higher values reflect a less precise fit. See ref 17, p 142. ^e Includes the spring energy contribution. ^f No fitting constraints applied. ^g Total-spring-relaxed energy; the difference in energy between fit and relaxed versions. ^h RMS values for a least-squares fit (MULTIFIT procedure *not* used) of the relaxed versions to a reference molecule (6) in the geometry that resulted from its participation in the initial multifit analysis.

of the receptor interactions for these two classes of compounds. Finally, these pharmacophore models were used in the prioritization of synthesis of existing targets, and in the design of a number of novel antagonists encompassing increased structural rigidity and lipophilicity.

Agonist Pharmacophore Model. In general, potent agonists (and antagonists) contain a primary or secondary basic amine and proximal and distal acidic groups. Structure-activity data demonstrate that a carboxylic acid is preferred for the proximal acid; the location and nature of the distal acid may be varied. Initially, it was hypothesized that NMDA agonists were interacting at a common receptor site and that the basic amine and two acidic groups were interacting with the same amino acid residues within that site. To test this assumption, a common orientation of the nitrogen, its lone pair, the α -CO₂H, and the distal acidic group within known agonists (Table I) was sought.

The cyclic agonists PDA (10–12), QUIN (13), and HOMOQUIN (14) were selected for initial studies. We felt that if the amine and acidic groups could be superimposed among these relatively rigid structures, then this would serve to define pharmacophoric relationships that could guide the superposition of the more flexible agonists in Table I. Upon construction of these agonists using SYBYL,¹⁵ we quickly came to the conclusion that the only way to superimpose all three moieties was to overlay the amine, α -CO₂H, and the distal acidic hydroxyl oxygen. This resulted in the ketonic oxygen of the distal acidic group occupying different areas of space for 10 and 11 (Figure 1). We therefore refined our initial hypothesis to state that only a distal acidic hydroxyl was necessary to interact with a common receptor residue.

The observation that analogues containing nonplanar distal acidic groups such as PO₃H₂ or SO₃H are either less potent, inactive, or antagonists^{8,16} led to the additional hypothesis that the acidic groups common to potent agonists must be able to reside in the same planes. To test these hypotheses, each agonist in Table I was built within SYBYL from available fragments using default bond lengths and angles, and the energy was minimized using MAXIMIN¹⁷ (default convergence criteria employed), without charges.¹⁸ After orienting the molecules with the basic nitrogen at the origin, the α -methylene along the x axis, and the carbon of the proximal CO₂H group in the x - y plane, two 2-Å tensors were defined that were perpendicular to the planes of the proximal and distal acidic groups, piercing through their hydroxyl oxygens (Figure 2). These tensors not only serve to record the positions of the proximal and distal acidic hydroxyls in space, they also allow one to incorporate

the (co)planar character of the acidic functionality during subsequent analyses. For cyclic analogues containing flexible rings, multiple ring conformations were examined using the RINGSEARCH algorithm within the SEARCH¹⁹ module of SYBYL. Low energy conformations (≤ 4 kcal/mol in energy variation, roughly the energy stabilization from a hydrogen bond) that presented the distal acidic group closest to that of more rigid agonists such as QUIN (13, Table I) were selected for further study.

By using the MULTIFIT¹⁷ procedure (intramolecular spring force constants of 20 kcal/mol Å² on all atoms employed in fitting), the structures in Table I were constrained to superimpose the endpoints of the tensors (Figure 2, Du atoms), together with the basic nitrogen and its lone pair (LP atom). Charges were not included in the calculations.¹⁸ For the cyclic analogues 10–12 and 16, axial and equatorial positioning of the amine hydrogen were employed in the fitting process, in successive runs. Because axial positioning of the hydrogen gave lower RMS fit values, these versions were used in the development of the pharmacophore model. Each constrained conformation resulting from the MULTIFIT procedure was then allowed to relax by rerunning MAXIMIN (without charges, using default convergence criteria) without any fitting constraints. In addition, conformational searches¹⁹ were run on the side chains containing the distal CO₂H group (0 to 360° scan at 30° increments of the bonds between the α -carbon of the amino acid and the distal CO₂H group) within the flexible agonists 5–9 to check that no conformers substantially (>4 kcal/mol) lower in energy were missed in the fitting process. None were found. By comparing conformations and energies with and without the fitting constraints, an assessment could be made of the degree of conformity of the pharmacophoric groups within each agonist to the consensus conformation that emerged from the MULTIFIT analysis.

The results are shown in Figures 3 and 4. With a few exceptions noted below, the agonists could be multifitted with low to moderate costs in energy (generally less than 3 kcal/mol). The quality of the superposition was evaluated by the RMS deviation between fit atoms and the spring energy (Table I; higher values mean a less precise fit). The total energy of the fit version (E_{total} ; includes the intramolecular spring energy, E_{spring}) and the energy of the relaxed form, $E_{relaxed}$ (minimized with no fitting constraints), also appear in Table I. Finally, the cost in internal energy (E_{cost}) was estimated for each molecule by comparing the energy of the putative receptor bound conformation (E_{total}) and the energy of the relaxed version ($E_{relaxed}$). We considered this difference in energy to be only an indication of the possibility for a given molecule to exist in the receptor bound conformation.

Several of the cyclic structures (16, D-KA; 17, D-IBO; 18, D-AMAA), as well as 7 (L-GLU), had significant total

(15) Commercially available from Tripos Associates, Inc., 1699 S. Hanley Road, St. Louis, MO 63144. Version 3.5, operating on a VAX 11/785, was used for the calculations. Version 5.3.2 was used to generate the figures.

(16) Watkins, J. C.; Olverman, H. J. *Trends Neurol. Sci.* 1987, 10 (7), 265.

(17) (a) Labanowski, J.; Motoc, I.; Naylor, C. B.; Mayer, D.; Dammkoehler, R. A. Three-Dimensional Quantitative Structure-Activity Relationships. 2. Conformational Mimicry and Topographical Similarity of Flexible Molecules. *Quant. Struct.-Act. Relat.* 1986, 5, 138. (b) The MULTIFIT option within MAXIMIN adds an extra potential, E_{mult} , which is minimized along with the structure, at some cost in conformational energy. The initial MULTIFIT analyses did not employ a reference structure to which the other molecules were fit. Rather, all molecules were allowed to fit each other simultaneously, resulting in a "consensus conformation" (multifit cluster). The RMS deviations resulting from this fit (Table I) were then calculated from an arithmetic mean of the coordinates of the fitting atoms.

(18) Because the goal of the agonist modeling analysis was to gain a qualitative feel if a working hypothesis about a pharmacophoric relationship between functional groups was operative (i.e., could a steric fit be achieved without unduly distorting valence and torsion angles), we felt it was inappropriate to include charges at this stage. Added to this was the difficulty of placing meaningful charges on the agonists based on in vacuo calculations, without a priori knowledge of the nature of the interactions between agonists and active site residues (or solvent molecules). Such interactions would undoubtedly affect the intramolecular electrostatic interactions, possibly screening negatively charged atoms within the agonists from each other.

(19) Dammkoehler, R. A.; Karasek, S. F.; Berkley Shands, E. F.; Marshall, G. R. Constrained search of conformational hyperspace. *J. Comput.-Aided Mol. Design* 1989, 3, 3–21.

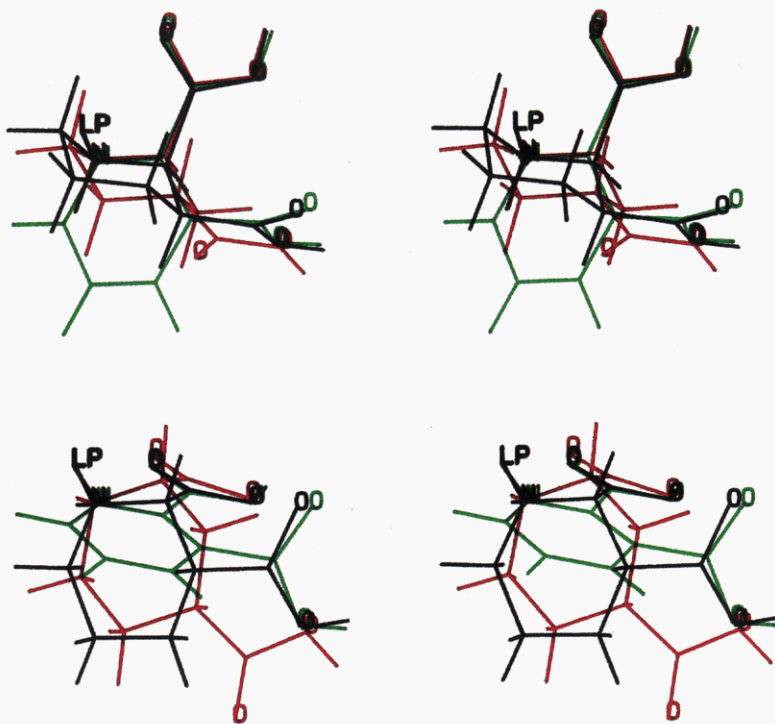


Figure 1. Orthogonal stereoviews of the initial superposition of the basic amine, α -CO₂H, and distal acidic hydroxyl oxygen of the cyclic agonists PDA (10, black, and 11, red) and QUIN (13, green). Note the projections of the ketonic oxygen atom of the distal acidic group within 10 and 11 to different areas of space.

and spring energies. When the fit conformations of 7 and 16–18 were relaxed using the MAXIMIN force field, their geometries changed only slightly, reflecting the introduction of significant ring strain and/or out of plane bending of the CO₂H in fitting.²⁰ Although a MULTIFIT analysis could have been rerun using lower intramolecular spring force constants, the fact that the relaxed structures could still present their pharmacophoric groups in close proximity to their positions as determined by the initial multifit analysis prompted us to do a simple least-squares fit (using the same atoms as were used in the MULTIFIT analysis above) of the relaxed geometries of 16–18 to a reference fit structure (compound 6) from the initial MULTIFIT analysis. The root mean square (RMS) value for the least-squares fit is shown in Table I beneath the RMS for the MULTIFIT version. No ready explanation is apparent for the relatively high cost of fitting 7 to the consensus multifit cluster. It is possible that its NMDA agonist activity is due in part to interaction with other subsites within the NMDA receptor complex. The relaxed version of 7 was also least-squares fit to the fit version of a reference molecule (6); the RMS value for this fit appears below the RMS of the MULTIFIT version.

The proposed agonist pharmacophore model is characterized by a folded conformation in which the planes of the acidic moieties are well defined (Figure 4), thereby positioning these moieties to interact with complementary functionalities at the receptor site. The two acidic groups fall within an average distance separation of 3.5–4 Å (Figure 5), and their planes are inclined 60° relative to each other. They each position an oxygen atom that can engage

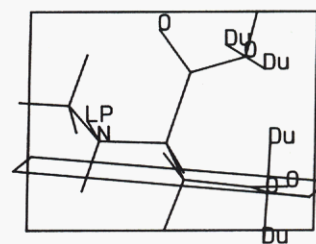


Figure 2. Plot of the fit conformation of NMDA (6), showing the planes defined by the acidic groups and the tensors normal to them (Du atoms) piercing through the hydroxyl oxygens. Also shown is the nitrogen lone pair (LP atom) used in the fitting process.

into a hydrogen-bond interaction with a common receptor site. The tight superposition of the distal acidic hydroxyl but the varying location of the rest of the moiety argues against a charge delocalization between both oxygens of the acid and in favor of a specific hydrogen bond between the acidic hydroxyl and the receptor. A cut-away view of the composite volume occupied by the agonists is shown in Figure 4.

Competitive Antagonist Pharmacophore Model. Although competitive antagonists retain the amino acid portion and distal acidic group that is present in the agonists, the SAR associated with their distal acidic groups differs considerably. In general, potent antagonists contain a distal PO₃H₂ moiety whereas agonists prefer a CO₂H. Although antagonists such as 1 can readily line up their functional moieties on the agonist pharmacophore, they generally occupy additional volume due to their larger structures (Figure 6). Recent reports of relatively rigid, potent antagonists^{6b} provided the opportunity to test the assumption of a common binding mode with agonists through the derivation of a separate competitive antagonist pharmacophore model.

(20) Another possibility is that MAXIMIN as implemented in version 3.5 of SYBYL was not accurately parameterized to handle cyclic structures such as 16–18. It was known that small changes in geometry in structures of this type resulted in large calculated energy differences.

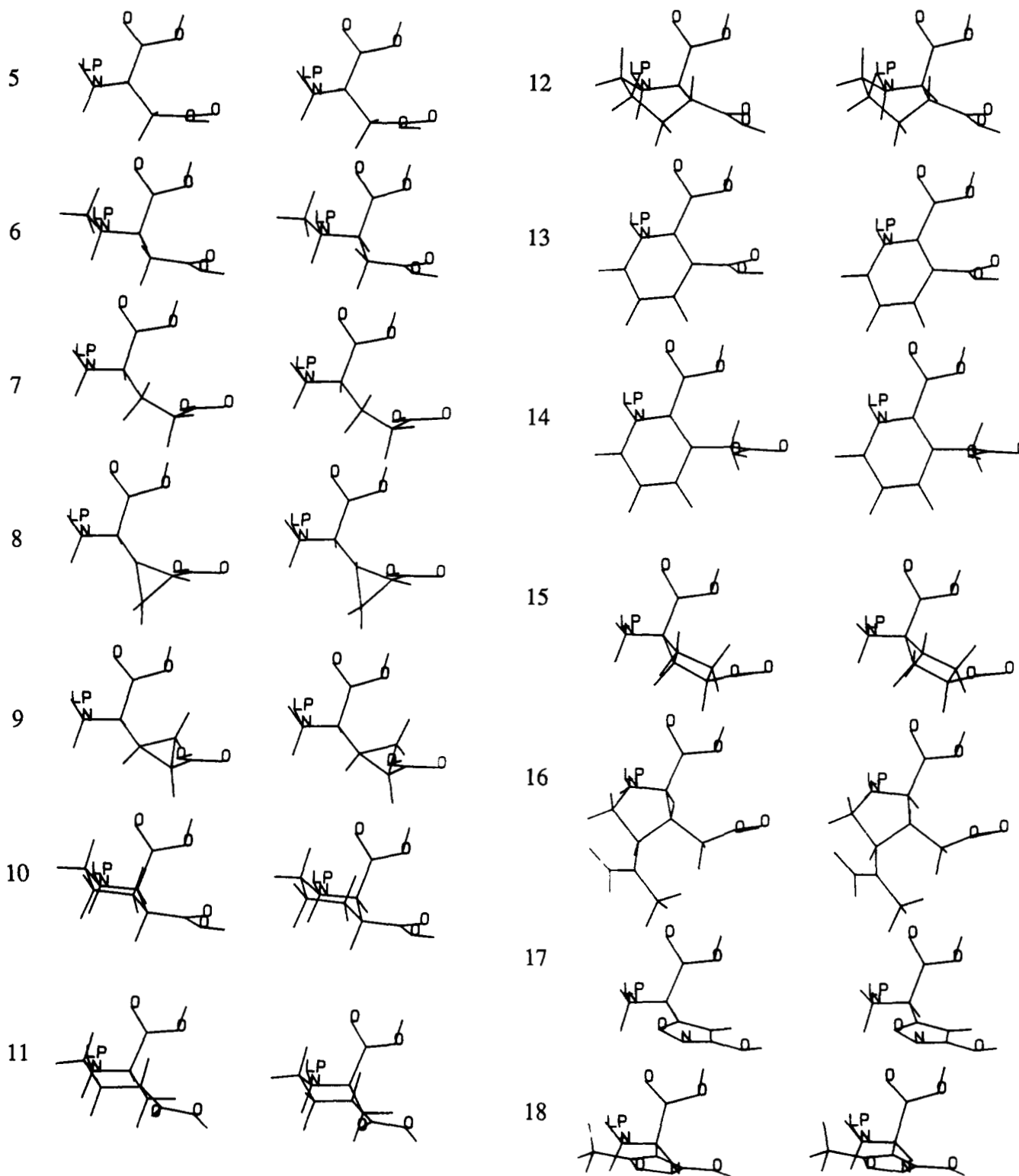


Figure 3. Stereoviews of the fit conformations of agonists used in the formation of the pharmacophore model: 5, L-ASP; 6, NMDA; 7, L-GLU; 8, D-CGA-C (2S,3R,4S); 9, D-CGA-D (2S,3S,4R); 10, PDA (*cis*-2R,3S; chair); 11, PDA (*trans*-2R,4R; chair); 12, PDA (*trans*-2R,3R; boat); 13, QUIN; 14, HOMOQUIN; 15, ADCP (*cis*-1R,3R); 16, D-KA (*trans*-2R,3R,4R); 17, D-IBO; 18, D-AMAA.

In examining known antagonists toward establishing an independent pharmacophore model, it became clear that a direct alignment of the basic amine, α -CO₂H, and PO₃H₂ groups would not be straightforward, because potent antagonists such as 1 and 2 possessed different side chain lengths. Therefore, under the assumption that the required basic amine and α -CO₂H within potent antagonists are binding to a common region of the receptor and thus can be overlaid, a receptor site interaction point was sought

to account for the distal acidic (CO₂H and PO₃H₂) groups. It was not assumed that this site point had anything in common with the previously defined agonist site point.

Geometry of PO₃H₂-Receptor Interactions. To better define a hypothetical receptor site point, literature data was screened to gain an understanding of the molecular geometry involved in the acceptor-donor interactions involving phosphonates. Although studies on PO₃H₂ hydrogen bonding preferences have appeared,²¹ no com-

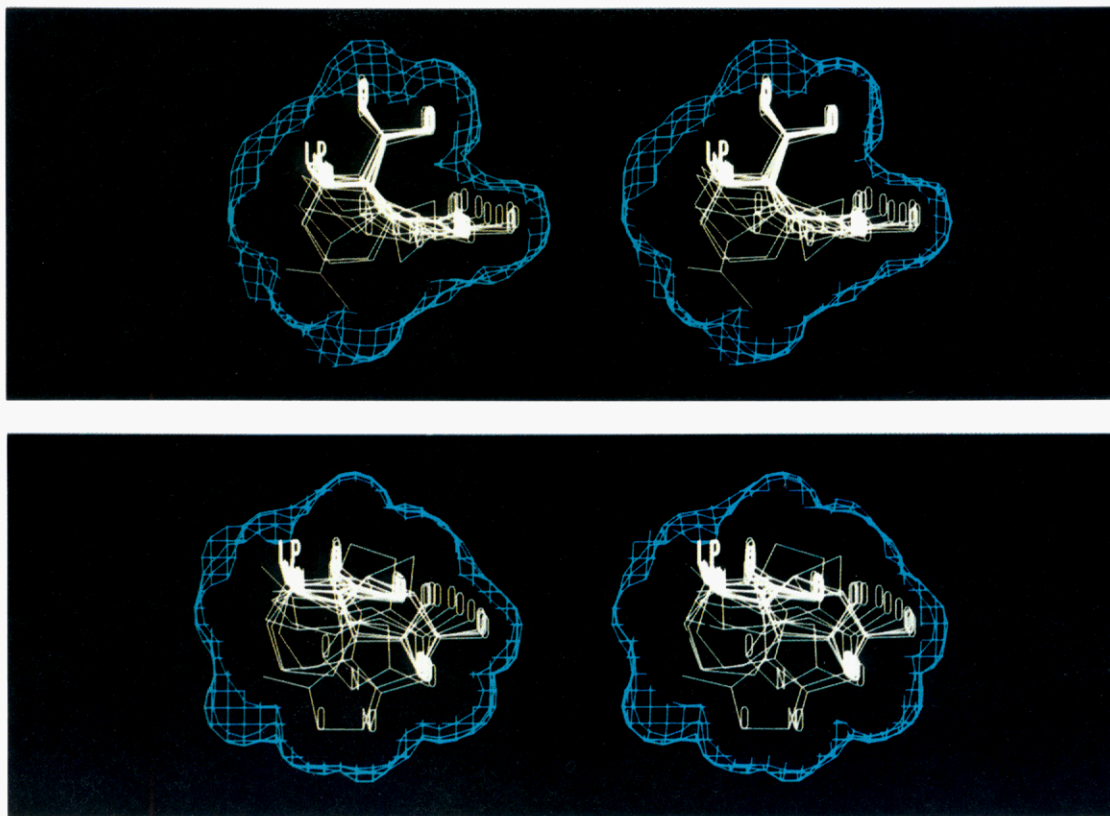


Figure 4. Orthogonal stereoviews of the superposition of the agonists from Figure 2 and Table I. Hydrogens have been removed for clarity. A cut-away view of the composite volume is shown in blue.

prehensive examinations of the geometry of PO_3H_2 -receptor interactions, such as was done with CO_2H ²² groups, have been reported. Therefore, both the Cambridge Structural²³ and Brookhaven Protein²⁴ databases were searched for $\text{PO}_3\cdots\text{X}$ (X = oxygen or nitrogen atoms) noncovalent interactions and the results combined to give

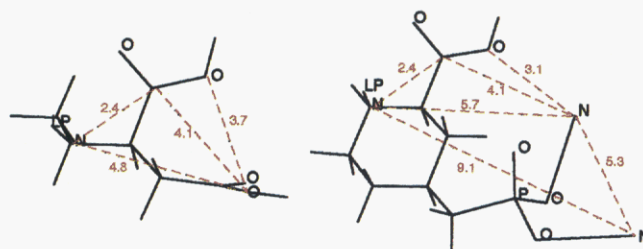


Figure 5. Distances between pharmacophoric groups in the agonist (left) and antagonist (right) models, illustrated using NMDA (6) and CGS 19755 (2), respectively, in their fit conformations. The nitrogen atoms attached to the PO_3 group represent receptor interaction points (see the antagonist modeling section of the text).

- (21) Alexander, R. S.; Kanyo, Z. F.; Chirlian, L. E.; Christianson, D. W. Stereochemistry of Phosphate Lewis Acid Interactions: Implications for Nucleic Acid Structure and Recognition. *J. Am. Chem. Soc.* **1990**, *112*, 933–937.
- (22) (a) Taylor, R.; Kennard, O. Hydrogen-Bond Geometry in Organic Crystals. *Acc. Chem. Res.* **1984**, *17*, 320–326. (b) Murray-Rust, P.; Glusker, J. P. Directional hydrogen bonding to sp^2 - and sp^3 -hybridized oxygen atoms and its relevance to ligand-macromolecule interactions. *J. Am. Chem. Soc.* **1984**, *106*, 1018–1025. (c) Vedani, A.; Dunitz, J. D. Lone-Pair Directionality in Hydrogen Bond Potential Functions for Molecular Mechanics Calculations: The Inhibition of Human Carbonic Anhydrase II by Sulfonamides. *J. Am. Chem. Soc.* **1985**, *107*, 7653–7658.
- (23) (a) Allen, F. H.; Kennard, O.; Taylor, R. Systematic Analysis of Structural Data as a Research Technique in Organic Chemistry. *Acc. Chem. Res.* **1983**, *16*, 146–153. (b) Allen, F. H.; Bellard, S.; Brice, M. D.; Cartwright, B. A.; Doubleday, A.; Higgs, H.; Hummelink, T.; Hummelink-Peters, B. G.; Kennard, O.; Motherwell, W. D. S.; Rodgers, J. R.; Watson, D. G. The Cambridge Crystallographic Data Centre: Computer-Based Search, Retrieval, Analysis, and Display of Information. *Acta Crystallogr.* **1979**, *B35*, 2331–2339.
- (24) (a) Bernstein, F. C.; Koetzle, T. F.; Williams, G. J. B.; Meyer, E. F., Jr.; Brice, M. D.; Rodgers, J. R.; Kennard, O.; Shimanouchi, T.; Tasumi, M. The Protein Data Bank: A Computer-Based Archival File for Macromolecular Structures. *J. Molec. Biol.* **1977**, *112*, 535–542. (b) Abola, E. E.; Bernstein, F. C.; Bryant, S. H.; Koetzle, T. F.; Weng, J. In *Crystallographic Databases-Information Content, Software Systems, Scientific Applications*; Allen, F. H., Bergerhoff, G., Sievers, R., Eds.; Data Commission of the Intern'l. Union of Crystallography: Bonn, 1987; pp 107–132.

average $\text{O}\cdots\text{X}$ distance and $\text{P}-\text{O}-\text{X}$ valence angle values of 2.8 ± 0.2 Å and $125 \pm 15^\circ$, respectively (see Tables VII and VIII and the Experimental Section).

Conformational Search Analyses. A hypothetical receptor atom was created that incorporated the PO_3H_2 -receptor site point geometry described above. Its energetically allowed positions in space relative to the NH_2 and $\alpha\text{-CO}_2\text{H}$ were then recorded as conformational searches of the flexible PO_3H_2 side chains of potent antagonists proceeded. By intersecting allowed positions of this receptor atom among potent antagonists, preferred location(s) in common were retained to define an antagonist pharmacophore model.

To accomplish this, the structures of an initial set of antagonists (Table II, top half) were built within SYBYL with extended side chains and rings in chair conformations, and minimized using MAXIMIN¹⁷ (no charges considered), using SYBYL default parameters.²⁵ Selection was based on available active compounds at the outset of the project, potency, and conformational rigidity. Compounds **22** and

Table II. Competitive Antagonists Used in the Initial Definition of PO₃H₂-Receptor Interaction Points^a

no.	IC ₅₀ , ^d μM	number of distances ^b		energies, kcal/mol ^c		
		unconstrained	constrained ^e	fit	relaxed	cost
2	0.054	378	—	-2.7	-3.3	0.3
1	0.082	2202	370	-0.5	-1.1	0.5
19 ^f	0.99	1186	275	3.3	1.3	0.9
20 ^h	0.66	1792	341	2.8	1.9	0.3
21 ⁱ	0.85	353	194	-1.3	-1.7	0.1
22 ^j	2.2	4199	375	-0.1	-1.1	0.4
96 conf. A conf. B	2.7	99 112	25 19	11.6 <i>f</i>	11.4 7.7	0 <i>f</i>
23 ^f	>100	2464	297	<i>f</i>	<i>f</i>	<i>f</i>
24 ^f	>100	916	118	<i>f</i>	<i>f</i>	<i>f</i>
3 ^k	0.28			-0.8	-1.4	0.3
4 ^k	0.77			-0.8	-1.7	0.7
25 ⁱ	0.79			-2.2	-3.4	0.5
26 ^m	1.6			2.6	-0.3	1.9
27 ^f	2.8			-0.1	-1.7	1.3
28 ^j	1.2			1.9	0.8	0.7

Table II (Continued)

no.	IC ₅₀ , ^d μ M	number of distances ^b		energies, kcal/mol ^c		
		unconstrained	constrained ^e	fit	relaxed	cost
29 ^j	5.2			2.0	0.1	0.6
30 ⁿ	5.6			-6.0	-7.6	0.4

^a Structures above the line were used to define the location of the receptor interaction points. Structures below, synthesized during the course of the search analysis, were added to the initial MULTIFIT to more precisely define the locations of the receptor interaction points and to evaluate the energetics of fitting. ^b See Figure 8 for an explanation of the distances employed. ^c See Table I for an explanation of the energies. Since the RMS deviation between fit atoms was <0.1 Å and the spring energy <1.3 kcal/mol for the compounds in this table, these values were not included. ^d For displacement of [³H]CPP from rat brain membranes; see the Experimental Section. ^e Searches were constrained to match the set of 378 distances from the search on 2. ^f Not used in the initial MULTIFIT analysis. ^g Reference 11. ^h Reference 50. ⁱ Reference 51. ^j Reference 52. ^k References 5, 43. ^l Reference 10a. ^m Tested as a mixture of stereoisomers; modeled structure was 2*R*,1'*R*,3'*S* isomer. See ref 53. ⁿ Prepared by hydrogenation of 116 with PtO₂ at 50 psi and 25 °C, followed by hydrolysis in 6 N HCl at reflux.

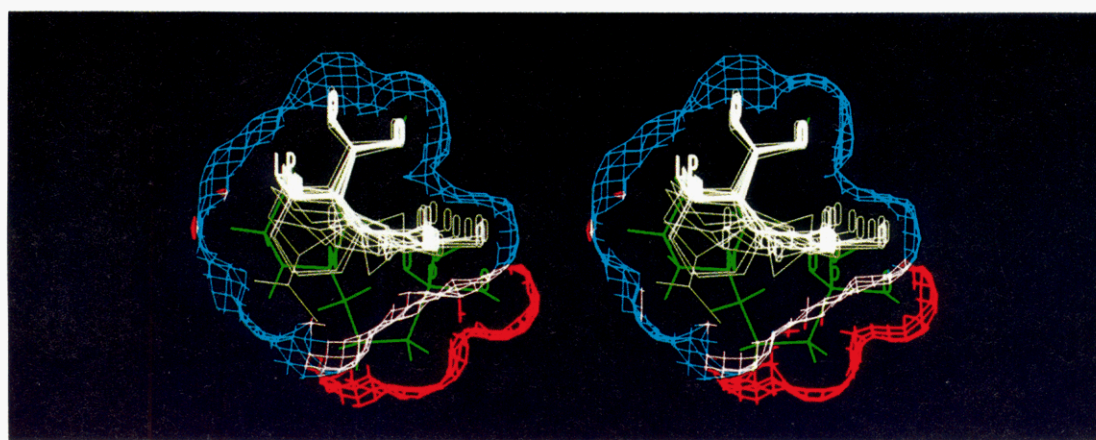


Figure 6. Stereoview of the fit of CPP (1, green) onto the agonist pharmacophore model, in a low energy conformation as determined by a conformational search analysis (see the antagonist modeling section for details). Hydrogens have been removed from the agonists for clarity. In red is shown the volume occupation of the PO₃H₂ side chain of CPP outside the composite volume of the active agonists.

96, although somewhat less potent, were included since it was felt that their reduced potency was due to factors other than the ability of their distal acidic groups to reach a receptor site point. Specifically, the decreased affinity of 22 could be due to increased entropy and possibly excluded volume, while 96 possessed a phosphonate directly bonded to an aryl ring, a substitution previously found to decrease affinity.²⁶

Consistent with literature data on CPP²⁷ (1) and AP5 (3),² which demonstrated that the *R* stereoisomer at the α -carbon of the amino acid portion was preferred for high affinity, antagonists were built with this atom in the *R* configuration. Because *cis*-2,4-disubstitution of the cy-

clohexane ring on antagonists such as 2 was favored over *trans* (Table III; compare the affinities of 2 and 33), building the cyclic analogues in the 2*R* configuration resulted in an *S* configuration at the 4-carbon. Therefore, antagonists containing a six-membered saturated rings were constructed as the 2*R*,4*S* isomer.

Charges were then calculated using the CNDO/2^{28,29} method. A hypothetical receptor site point (an sp³ nitrogen atom) was added to one of the PO₃H₂ hydroxyl oxygens in the geometry defined by the database searches above, replacing that hydroxyl's hydrogen (Figure 7). A nitrogen atom was chosen because it was felt this would be the smallest heavy atom in a receptor one would normally expect the PO₃H₂ group to hydrogen bond to. Therefore, in a conformational search setting, use of a van der Waals radius of a nitrogen atom would allow the most conformations to be selected (not rejected due to intermolecular

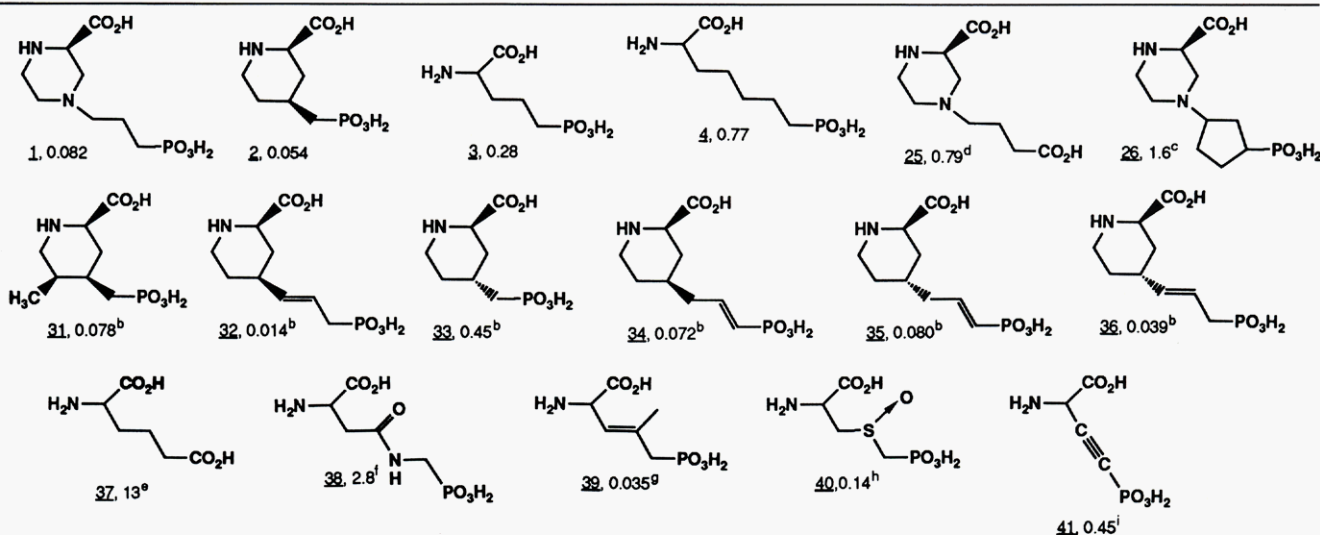
(25) Parameters were unavailable for the C.ar-P.O3 (aromatic carbon to phosphonate phosphorous atom) bond present in several of the antagonists. Stretching, bending, and torsional parameters for a C.2-P.O3 (C.2 = an sp² carbon atom) bond were substituted, and a C.ar-P.O3 equilibrium bond length of 1.76 Å was determined by searching the Cambridge Structural Database²³ for occurrences of C.ar-P.O3 pairs and averaging the resulting bond lengths.

(26) For examples, see refs 10a, 11, and 52b.

(27) Aebischer, B.; Frey, P.; Haerter, H.-P.; Herrling, P. L.; Mueller, W.; Olvermann, H. J.; Watkins, J. C. Synthesis and NMDA Antagonistic Properties of the Enantiomers of 4-(3-Phosphonopropyl)piperazine-2-carboxylic acid (CPP) and of the Unsaturated Analogue (E)-4-(3-Phosphonoprop-2-enyl)-piperazine-2-carboxylic acid (CPP-ene). *Helv. Chim. Acta* 1989, 72, 1043-1051.

(28) (a) Pople, J. A.; Beveridge, D. L. *Approximate Molecular Orbital Theory*, McGraw-Hill: New York, 1970. (b) Structures were passed from SYBYL to CHEMLAB-II²⁹ (version 10.0) for charge calculations using the CNDO/2 module. Density matrix-derived point charges were used in the calculations. The MOL2 files in the supplementary material contain atomic charges for selected compounds.

(29) (a) Pearlstein, R. A. *CHEMLAB-II Reference Manual*; Chemlab, Inc. (software available from Molecular Design Limited, San Leandro, CA). (b) Childress, T., Ed. Revised MDL Edition, March 1985; Molecular Design Limited, San Leandro, CA.

Table III. Antagonists Used To Define the Receptor-Tolerated Volume^a

^a See Figure 13. IC₅₀'s (μ M) are given after the compound number. A table of fitting energies is included in the supplementary material. ^b Reference 6b. ^c Reference 53b; also see footnote m of Table II. ^d Reference 10a. ^e Reference 2a. ^f References 54, 55. ^g Reference 56. ^h Reference 57. ⁱ Reference 58.

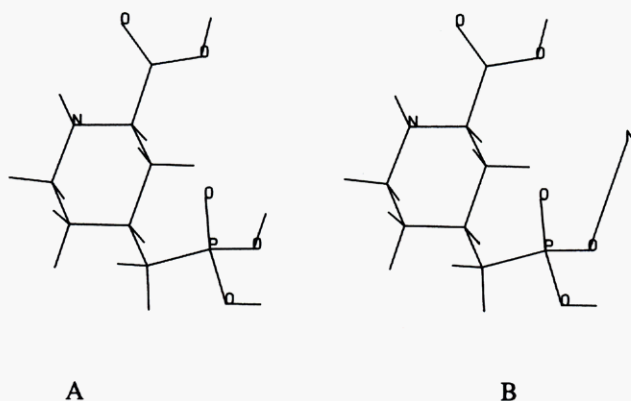


Figure 7. Structure of CGS 19755 (2). Version A is the standard molecule as initially constructed and minimized, and version B contains a hypothetical receptor (a nitrogen) atom 2.8 Å from and bonded to one of the PO₃H₂ oxygen atoms.

steric contacts). After superimposing the basic amine, its lone pair, and the proximal CO₂H, conformational searches were run on the PO₃H₂ side chains (SYBYL, SEARCH¹⁹ procedure); see the Experimental Section for details. Two methods of recording the position of the receptor site point were investigated. The coordinate map approach (termed vector maps in version 3.5 of SYBYL) failed due to size limitations (the maximum number of vectors that could be recorded [2000] was exceeded in unconstrained searches on molecules such as 1); the distance map method (termed orientation maps in version 3.5) proved successful in recording allowed receptor atom locations.

By intersecting allowed distances among the active antagonists 1, 2, and 19–22 (Table II, Figure 8) and then subtracting distances corresponding to the inactive analogues 23 and 24, a set of 17 distances resulted that corresponded to 25 conformations of 2 (Figure 9). Intersecting the search results of 96, a compound that was synthesized after the initial analysis was completed, further constrained the results to a single set of distances (with several near misses) that mapped out a unique area of space for the receptor interaction atom (Figure 10). A representative set of distances from this area was chosen as the location of a receptor interaction, hereafter referred to as the "primary receptor interaction point" (Figure 11).

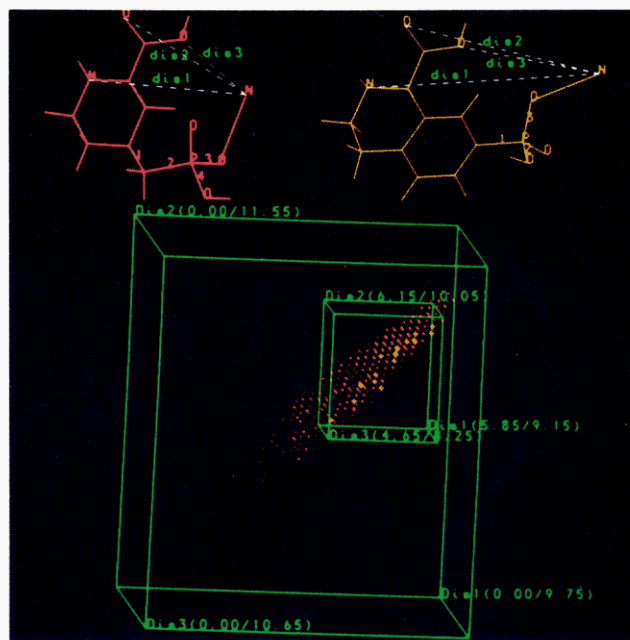


Figure 8. Overlay of distance map recordings for the unconstrained search of CGS 19755 (2, red; 378 distances; see Table II) and a constrained search of 96 (yellow; 19 distances). The bonds that were scanned in the search analysis are numbered.

On fitting the active antagonists 1, 2, 19–22, and 96 to this point, a "secondary" receptor interaction point was defined that was capable of a hydrogen-bonding interaction with the other hydroxyl group within the PO₃H₂ moiety, or a lone pair attached to the ketonic oxygen atom of those antagonists containing a distal CO₂H moiety (Figure 12). The third (ketonic) oxygen, while projecting a negative electrostatic potential to the north and northwest portion of the structures as they appear in Figures 9 and 10, did not suggest the formation of a hydrogen bond with a specific receptor atom due to its varying spatial occupation among potent antagonists.

To locate more precisely the primary and secondary receptor interaction points, as well as evaluate the relative energetics of the fit versus relaxed conformations, the fit

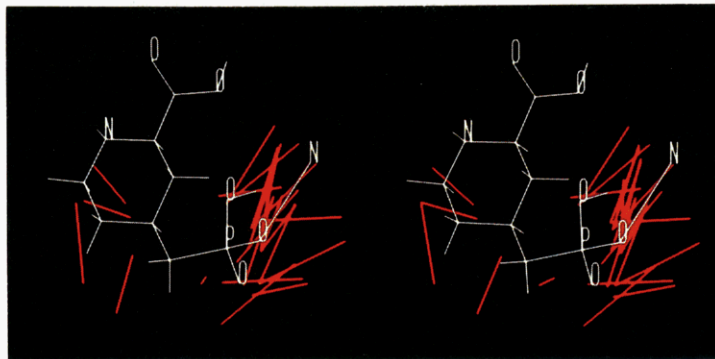


Figure 9. A recording of the P...X (X = an sp^3 nitrogen atom used to represent a receptor interaction) bond (red lines) from the 25 conformations of 2 that could reach the 17 distances resulting from the initial analysis of 1, 2, and 19–24 (Table II).

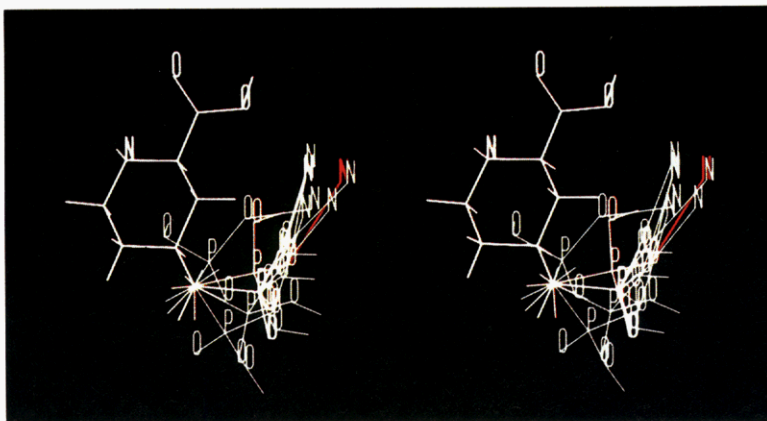


Figure 10. Remaining conformations of 2 after the search results of 96 (both ring conformers) were intersected. The conformer chosen for the initial receptor-site location is shown in red.

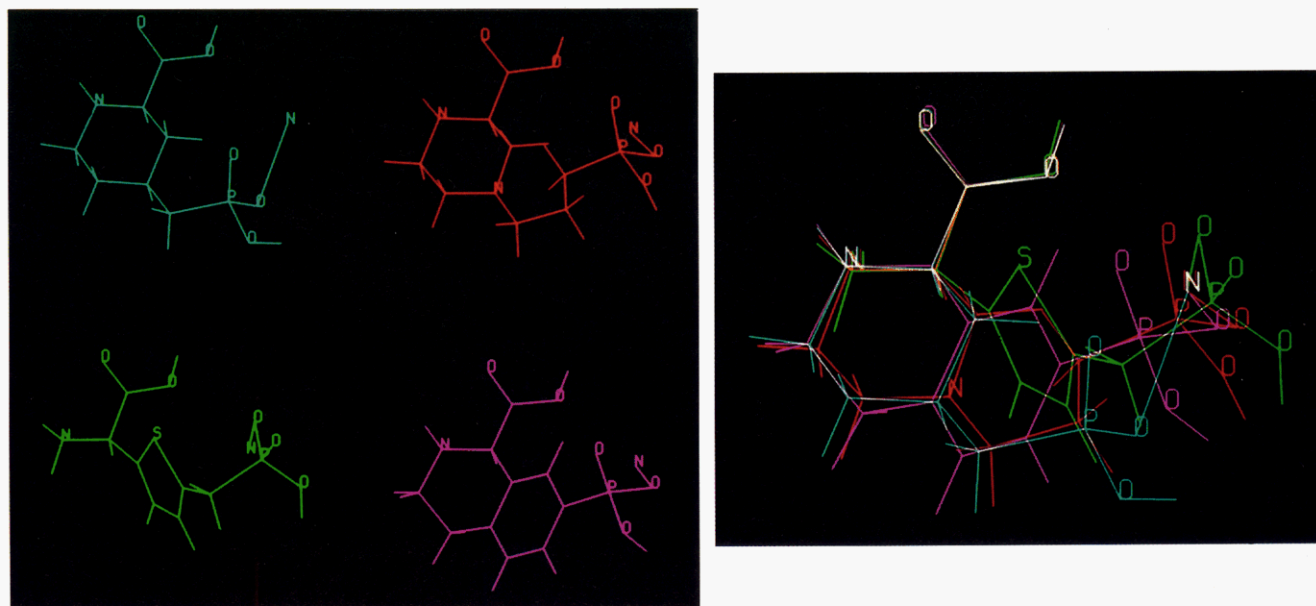


Figure 11. Fit conformations of 1 (red), 2 (aqua), 20 (green), and 96 (purple) (left), and their overlay (right), showing the alignment of the primary receptor interaction point (white N atom).

versions of 1–4, 19–22, 96, and additional active compounds 25–30, synthesized during the course of the search analyses, were subjected to a MULTIFIT¹⁷ analysis. Similar to the analysis involving the agonists, the structures were built, minimized using MAXIMIN, and oriented with the basic nitrogen at the origin, the α -methylene along the x axis, and the carbon of the proximal CO_2H group in the x - y plane. A 2-Å tensor was defined that was perpendicular to the plane of the proximal CO_2H , piercing through the hydroxyl oxygen. The structures were then constrained to superimpose the endpoints of this tensor, the basic

nitrogen, its lone pair, and the receptor interaction points. Intramolecular spring force constants of 20 kcal/mol Å^2 were used on all fitting atoms, except for the secondary receptor interaction point. The spring force constant for this atom was reduced to 10 kcal/mol Å^2 to reflect the somewhat reduced importance of interaction with this site for maintenance of high affinity to the NMDA receptor.³⁰ Charges were not included in the calculations. After running MULTIFIT, the structures were allowed to relax by rerunning MAXIMIN (without charges) on the multifit geometry without any constraints.

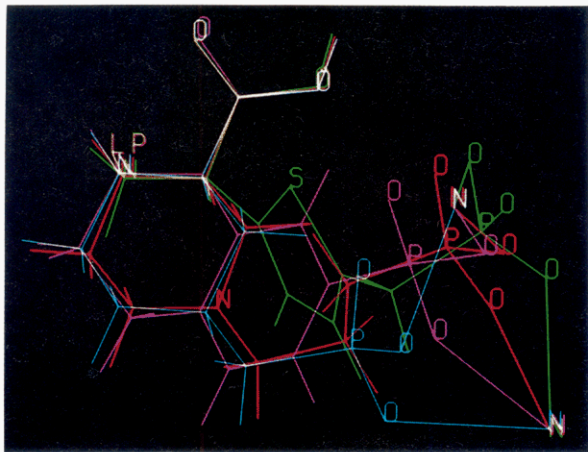


Figure 12. After fitting, it was noted that a secondary interaction point near the other PO_3H_2 hydroxyl group could be defined.

Volume and Electrostatic Computations. Additional antagonists synthesized in our laboratories or reported in the literature subsequent to the initial MULTIFIT analysis were then added to the model by multifitting them to a reference fit compound, **2**, and evaluating the energetics of the fit versus relaxed versions. In this manner, approximately 100 structures were added to the model. Selected compounds that were used in the computation of the receptor-tolerated volume (Figure 13, blue area) appear in Table III. Selection was based on volume contribution—active analogues that did not occupy additional volume outside the composite volume of the structures in Table III were not included.

In general, less potent potent analogues fell into four main categories: (1) those with excluded volume (Tables IV and V); (2) those that lack key structural features such as an $\alpha\text{-CO}_2\text{H}$ or a primary or secondary basic amine (**85**, Chart I, and **57**, Table V, respectively; compare both with **1**, Table II); (3) those that could not reach one or more of the distal acidic receptor interaction sites (Table II, **23** and **24**); and (4) those with an electrostatic potential pattern different from that exhibited by potent antagonists in key regions (**86**, Chart I; also, **81** and **83**, Table VI; Figure 14). In Table IV are listed compounds used in the computation of volume corresponding to roughly a 10-fold decrease in potency (Figure 15, yellow volume), while structures corresponding to severe receptor excluded volume (>100 fold decrease in potency) appear in Table V (Figures 15 and 16, red volume). Compounds falling into categories 1 and 4 all possessed the key structural features necessary for high affinity and could reach the receptor interaction sites with a minimal energy cost, yet remained markedly less potent.

CNDO/2 charges²⁸ and electrostatic potentials³¹ were calculated for all antagonists fit to the model. Beyond the generally negative (proton attractive) potential associated

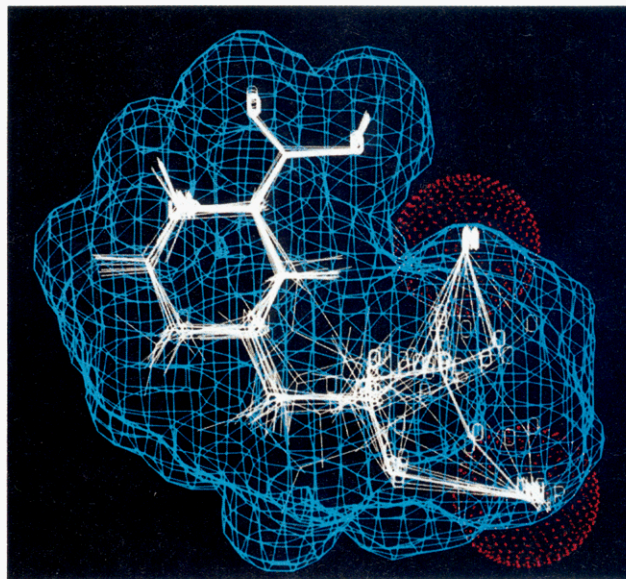


Figure 13. Superposition of 17 potent antagonists (Table III), the composite receptor-tolerated volume (blue), and the receptor-site atoms (white N atoms or lone pair [LP] electrons surrounded by red dots). Lone pairs were used for the receptor-site atoms being interacted with by the ketonic oxygen atom within those antagonists containing distal CO_2H groups (see text).

with the PO_3H_2 and $\alpha\text{-CO}_2\text{H}$ groups and the neutral to positive potential connected with the lipophilic portions of the structures, a key feature involved the electrostatic potential associated with the third (ketonic) oxygen of the PO_3H_2 group. Although a specific hydrogen bonding receptor interaction point for this atom could not be defined, the presence of this potential and the direction of its projection appeared to be related to antagonist potency. For example, antagonists possessing a distal CO_2H instead of a PO_3H_2 moiety were 10-fold less potent, presumably because they lack this negative potential. Although these analogues could be less potent because they lack volume corresponding to the third oxygen atom of the PO_3H_2 , the phosphinic analogue of **1**, which places a methyl group in the same location as the third (ketonic) PO_3H_2 oxygen, is also approximately 10-fold less potent ($\text{IC}_{50} = 0.78 \mu\text{M}^{10a}$).

When AP6 (**81**) and **83** were fit to the model, the ketonic PO_3H_2 oxygen atom projected a negative potential toward the basic amine (Figure 14), which was reflected in part by a larger X component of the dipole moment as calculated via CNDO/2²⁸ (Table VI, compare μ_x for **3**, **81**, and **4**). This potential may inhibit the approach of a negatively charged receptor atom that must interact with the amine for strong binding. The periodicity in affinity as the PO_3H_2 side chains are lengthened in the AP4-5-6-7 (**80-3-81-4**) and **82-83-1-84** series (Table VI) can be rationalized by this observation.

Results. Similar to the agonist model, the competitive antagonist pharmacophore model entails a folded conformation and contains two specific receptor interaction points off of the distal phosphonic acid (Figures 6 and 17). Both points are roughly in the plane of the piperazine ring of **1**, and one is positioned such that a receptor moiety could simultaneously hydrogen bond to oxygens on the PO_3H_2 and $\alpha\text{-CO}_2\text{H}$ groups. This point is also in proximity to the distal acidic hydroxyl of the agonist model described above. Similar to other models,^{2,6b} strict volume requirements are found near the basic amine, α to the phosphonic acid, and surrounding the receptor interaction sites (Figure 14), presumably reflecting critical receptor interactions occurring in these areas. However, some volume tolerance

(30) From the SAR/modeling analyses, there were examples (compounds **37**, **51**, **52**, and **80**) of compounds that, when fit to the "primary" receptor interaction point at the appropriate hydrogen bond length (2.8 Å) and P–O–N valence angle (125°), could not be made to form a strong hydrogen bond with the "secondary" interaction point in a low energy conformation (wrong distance and/or valence angle). These compounds were 10–100x less potent than closely related analogues (**3** and **19**) that could interact with this site at the appropriate geometry. However, compounds (such as **23** and **24**, Table II) not capable of interacting with the "primary" interaction site at the appropriate geometry were markedly less potent (>1000x loss in affinity).

Table IV. Antagonists Used To Define Moderate Receptor-Excluded Volume^a

No.	R ₁	R ₂	R ₃	R ₄	IC ₅₀ (μM) ^b
42	CH ₃	H	H	H	1.3
43	H	CH ₃	H	H	1.6
44	H	H	CH ₃	CH ₃	1.3
45(R)	H	H	CH ₃	H	} 0.8
46(S)	H	H	CH ₃	H	

47, 10 μM ^c	48, 48 μM ^d	49(R), 5.8 μM ^{d,e}	50, 32 μM ^f	51, (D-3C-PG), 25 μM ^d	52, >100 μM ^h	53, 5.9 μM ^f	54, 50 μM ^f	55, ~50 μM ^k	56, >100 μM ^{k,l}

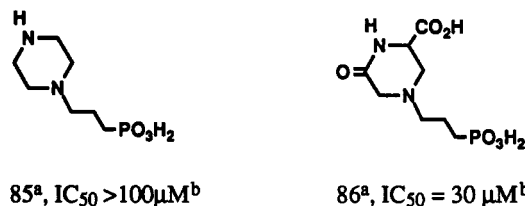
21, 0.85 μM	22, 2.2 μM ^m	23, 5.2 μM ^m	24, 2.8 μM ^h	25, 2.8 μM ^h	26, 2.7 μM	27, 0.77 μM	28, 2.8 μM ^h	29, 2.2 μM ^m	30, 5.6 μM

^a Volume, that if occupied, results in approximately a 10-fold decrease in affinity (Figure 15). IC₅₀'s (μM) are given after the compound number. A table of fitting energies is included in the supplementary material. ^b Reference 6b. ^c Reference 58. ^d Reference 10a. ^e Tested as a 1:3 mixture of isomers. ^f Reference 53b. ^g Reference 16. ^h Reference 11. ⁱ Reference 50. ^j Reference 59. ^k Reference 60. ^l The reduced potency of this analog was felt to be due primarily to adverse electronic effects conferred by the NH₂ proximal to the distal acid. ^m Reference 52.

was noted off of the 4–6 positions of the piperidine ring of **2** and to the front of the model (Figure 16). The presence of negatively charged, polar moieties near the basic amine diminish potency, possibly because they are hindering a critical NH to receptor interaction.

Comparison of Agonist and Antagonist Models. The main differences between the agonist and antagonist models are the significantly greater volume occupation by the larger antagonists, especially in the area of the phosphonate side chain, and the existence of a second receptor site near the distal phosphonic acid moiety for antagonists. The similar SAR and volume requirements surrounding the basic amine, α-CO₂H, and distal acidic receptor interaction point, coupled with the similar location in space

Chart I. Additional Examples of Less-Potent Antagonists



^a Reference 53b. ^b For displacement of [³H]CPP from rat brain membranes, see the Experimental Section.

of the primary receptor interaction point for both agonists and antagonists, derived by independent modeling approaches, argues that at least one face of the agonists and antagonists are binding to the same area of the NMDA receptor complex. Thus, one can hypothesize (Figure 18) that while agonists and antagonists interact with the same receptor groups off of one face of the structure, the larger antagonists are preventing a conformational change in receptor structure that is responsible for agonist activity.

Design of Novel Antagonists. An early objective of this work was to reduce the conformational flexibility of

(31) Molecular electrostatic potentials based on the point charges were contoured at +1, -1, and 5 kcal/mol above the minimum potential (default values within the POTENTIAL command in SYBYL). All antagonists were aligned with the basic amine at the origin, the α-carbon along the positive x-axis, and the carbon of the α-CO₂H in the positive x-y quadrant. The direction of projection of electrostatic potentials were relative to this invariant amino acid portion.

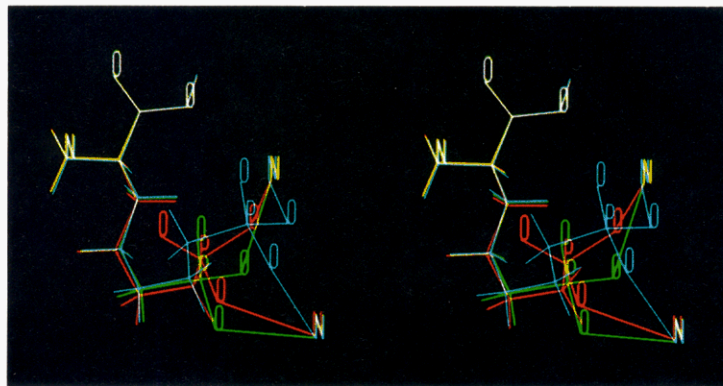
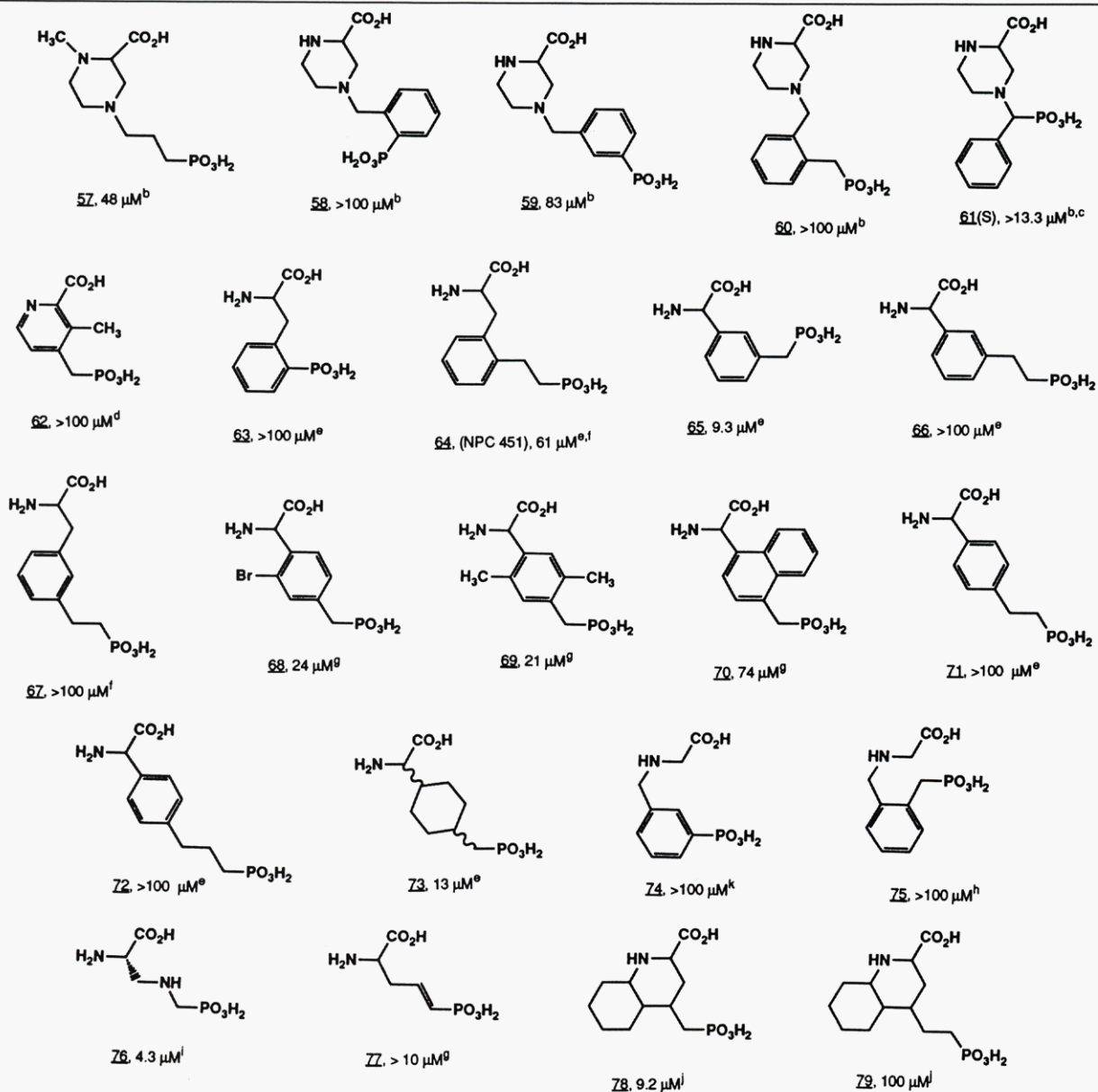


Figure 14. An overlay of the fit versions of 3 (green), 81 (red), and 4 (cyan). Note the direction of projection the ketonic PO_3H_2 oxygen atom (not bonded to the receptor interaction points). The active compounds 3 and 4 project to the north, while the less-potent analogue 81 projects to the northwest, toward the basic NH_2 . This is reflected by an increased value calculated for the x component of the dipole moment (see text).

Table V. Antagonists Used To Define Severe Receptor-Excluded Volume^a



^a Volume, that if occupied, results in a ≥ 100 -fold decrease in affinity (Figures 15 and 16). IC_{50} 's (μM) are given after the compound number. A table of fitting energies is included in the supplementary material. ^b Reference 10a. ^c Tested as a 1.6:1 mixture of isomers. See 49 in Table IV. ^d Reference 59. ^e Reference 11. ^f Reference 55. ^g Reference 61. ^h Reference 52. ⁱ Reference 57b. ^j Prepared by hydrogenation of the aromatic ring of the corresponding quinolines with PtO_2 at 50 psi and 25 °C; ref 51.

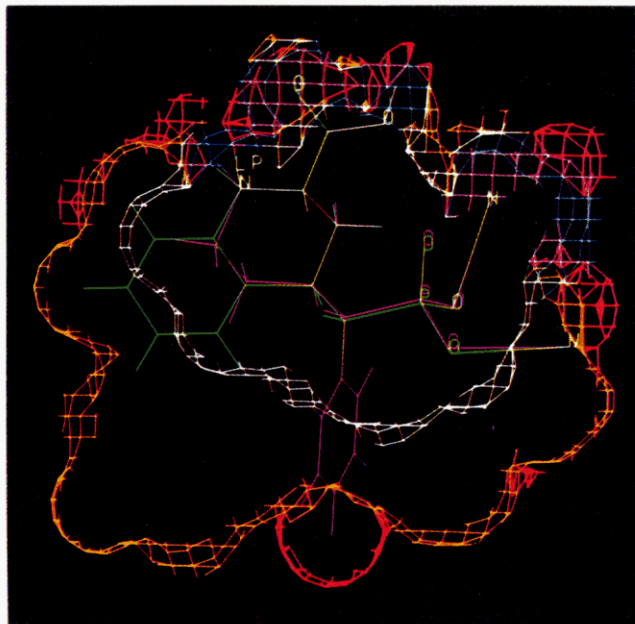


Figure 15. Cut-away view of a portion of the receptor tolerated (blue), moderate (yellow), and severe (red) receptor excluded volumes, with examples of less-potent analogues **21** (green) and **61** (purple) included. The interface between the receptor-tolerated volume and moderate receptor-excluded volume is colored white, and areas where all three volumes intersect is pink.

Table VI. Periodicity in Binding Affinity of Competitive Antagonists

no.	name	<i>n</i>	IC ₅₀ ^a μM	μ _x ^b	no.	name	<i>n</i>	IC ₅₀ ^a μM	μ _x ^b
80 ^c	AP4	2	>100	3.3					
3	AP5	3	0.28	2.6	82 ^d		1	0.32	2.0
81 ^c	AP6	4	42	5.4	83 ^d		2	9.8	3.7
4	AP7	5	0.77	1.1	1	CPP	3	0.082	0.7
					84 ^d		4	48	2.1

^a For displacement of [³H]CPP from rat brain membranes; see the Experimental Section. ^b X component of the dipole moment, in debyes, calculated from the density matrix via the CNDO/2²⁸ procedure. ^c Reference 2. ^d Reference 10a.

a previously reported series of aryl APH analogues.¹¹ Specifically, hybrid derivatives that combined the cyclic amino acid functionality present in known antagonists such as CGS19755 (**2**) and the phenyl spacer found in the aryl APH analogues were envisioned. One such combination involved phosphonoalkyl-substituted 1-carboxytetrahydroisoquinolines, where the alkylphosphonate side chain

Table VII. Results of Cambridge Structural Database²³ Search

refcode	<i>d</i>	θ	refcode	<i>d</i>	θ
ACETPA	2.63	120	HISAPH	2.69	126
ADPOSM	2.86	104		2.73	124
AFCYDP	2.75	127	IMDAZP	2.71	118
AGUAHP	3.09	115	IPRAZP	2.66	117
	2.90	114	LARGPH	2.84	125
AMAFAP	2.79	114	MGUANP	3.04	120
	2.77	116	MINOSP	2.90	108
AMPETP	2.80	119	PUTRDP	2.79	113
AZURPH	2.84	126	RBADPM	2.76	127
BALVAL	2.73	124		2.71	138
BORTAD	2.61	117		2.66	129
	2.61	104	THPPTH	2.73	138
CILHUA	2.41	124		2.83	120
CRBAMP	2.42	130		2.47	151
	2.98	107		2.46	119
DAZYAE	2.61	126		2.53	164
DOFJOX	2.70	120	TLPTUR	2.94	139
	3.30	126	URECAP	2.61	115
DUJPED	2.53	117		2.68	111
	2.51	117	DOPSUW	2.82	116
EPHDHP	2.81	135		2.56	140
ETHDPH	2.45	119	DUNHID	3.04	125
GLYCPH	2.59	112		2.94	108
GLYGLP	2.50	125			
HCCOXE	2.59	118	mean	2.73	122
	2.96	132	std dev	0.19	11
			N	49	49

Table VIII. Summary of Results of Brookhaven Protein Databank²⁴ Search^a

refcode	resolution, Å	number of interactions			
		side chain	backbone	water	total
1FX1	2.0	4	5	0	9
1GPD	2.9	0	2	0	2
1HHO ^b	2.1	1	0	0	1
2GRS	2.0	4	3	0	7
2MDH	2.5	2	5	0	7
2SNS	1.5	3	0	0	3
2TGD ^b	2.1	0	0	2	0
3DFR ^b	1.7	7	7	6	20
3FXN	1.9	4	5	0	9
3LDH	3.0	3	4	0	8
3PTP ^b	1.5	2	3	0	5
4FXN	1.8	5	7	0	12
5ADH ^b	2.9	1	1	3	5
5LDH	2.7	3	1	0	4
5RSA ^b	2.0	2	1	1	4
6ADH	2.9	4	6	0	10
7CAT ^b	2.5	2	1	1	4
8CAT ^b	2.5	3	2	0	5
grand total					122

^a A listing of individual observations and a statistical (frequency) analysis of the data can be found in the supplementary material.

^b X-ray contains solvent (H₂O) molecules.

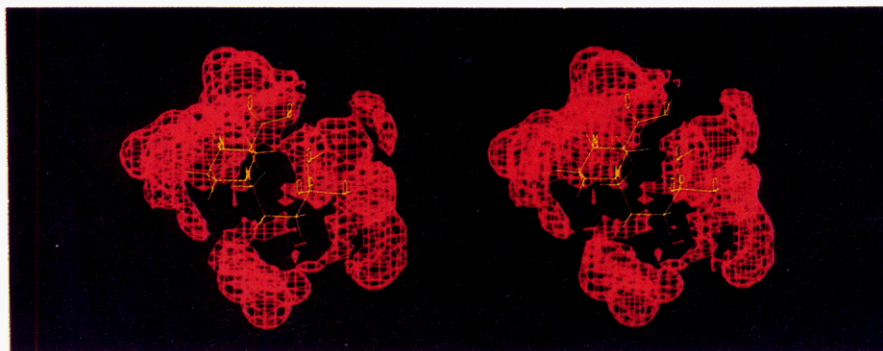


Figure 16. Stereoviews of the entire severe excluded volume, with the fit version of **1** included for reference.

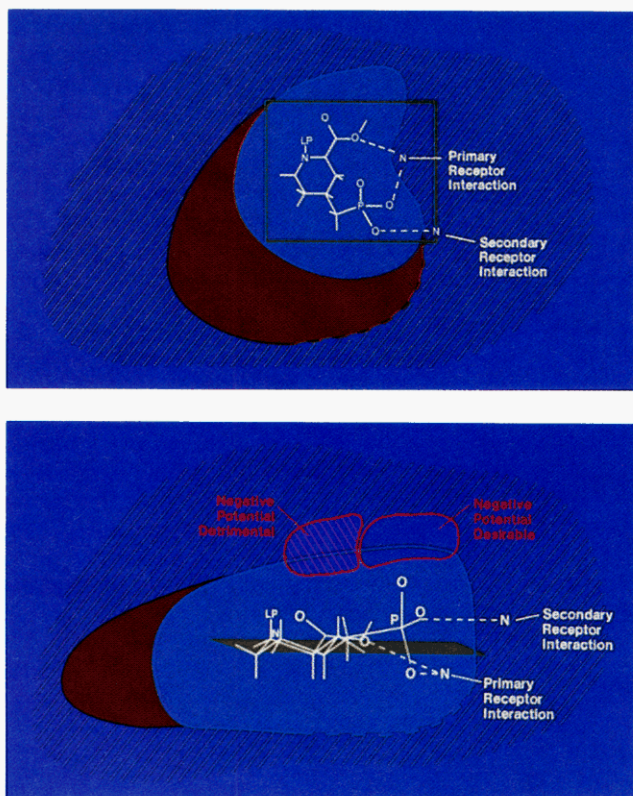


Figure 17. Summary of the NMDA competitive antagonist pharmacophore model, from two views (top-down and edge-on to the piperidine ring of **2**). The plane defined by the piperidine ring is shown in light green, and the receptor (active) volume appears in light blue (Table III, Figure 13).

has four possible sites of attachment on the aromatic ring. These analogues were selected initially on the basis of their synthetic accessibility. However, at this preliminary stage, prediction of optimum substitution patterns was difficult.

As the antagonist pharmacophore model developed, it became apparent that fusing an aromatic ring onto the 4 and 5 positions of the piperidine ring of **2** was sterically tolerated and would result in a relatively rigid, lipophilic³² 3-carboxytetrahydroisoquinoline ring system. Addition of phosphonoalkyl side chains at the appropriate ring position would then result in analogues capable of interacting directly with the two receptor interaction points in the appropriate hydrogen-bonding geometry, while remaining within the confines of the active-volume region. On the basis of the antagonist pharmacophore model, low energy conformations of the 5-substituted analogues were predicted to fulfill these criteria. Furthermore, knowledge of electronic requirements at the receptor suggested that the periodicity in affinity observed in the AP4-5-6-7 and 82-83-1-84 series (Table VI) would be mimicked by the alkyl homologues, 87-88-89.

The synthesis and a detailed discussion of the SAR of both the 1- and 3-carboxytetrahydroisoquinolines is described below. Figure 19 depicts the fit of one of the most potent analogues (**89**) in the competitive antagonist pharmacophore model.

Chemistry

In general, directly bonded aromatic phosphonic acids were prepared by palladium(0)-mediated coupling reac-

tions of aromatic bromides or triflates with diethyl phosphite.³³ In cases where a 2-phosphonoethyl fragment was desired, it was possible to utilize a palladium(II)-catalyzed coupling of an aromatic bromide or triflate with diethyl vinylphosphonate followed by hydrogenation of the double bond.³⁴ Incorporation of phosphonomethyl substituents was accomplished by displacement of an appropriately substituted benzyl bromide with sodium diethyl phosphite.

Initially, 1-carboxy-5- and 7-(phosphonoalkyl)tetrahydroisoquinolines were prepared by the route shown in Scheme I. Introduction of 5-phosphono or 5-phosphonoethyl substitution was accomplished by palladium catalysis of either bromo- or trifluoromethanesulfonyl-substituted isoquinolines. Introduction of the 1-carboxylic acid was effected by modified Reissert-Henze chemistry.³⁵ N-Oxidation of the isoquinoline with *m*-chloroperoxybenzoic acid followed by heating with trimethylsilyl cyanide and triethylamine afforded the nitrile, which was subsequently converted to an amide by heating in concentrated sulfuric acid at 90 °C. The amide intermediates were hydrogenated and then further hydrolyzed in refluxing aqueous 6 N HCl for 24-48 h to provide the target compounds.

A second method utilized for the preparation of phosphono- and phosphonoalkyl-substituted 1-carboxytetrahydroisoquinolines is illustrated in Scheme II. In this case, the intramolecular amidoalkylation reaction of ethyl [2- or 4-(bromophenyl)ethyl]carbamates (**123** and **124**) with glyoxylic acid provided the appropriately substituted 1-carboxytetrahydroisoquinolines.³⁶ A rather unexpected finding was the ease with which the ring brominated and presumably moderately deactivated phenethylamines cyclized,³⁷ since facile cyclization of an electron-deficient ring is unusual. Elaboration of the 7-bromoisoquinoline **126** to the phosphono and phosphonoethyl derivatives **96** and **98** proceeded smoothly. However, in the case of 5-bromotetrahydroisoquinoline **127**, palladium(0)-catalyzed phosphonate replacement proceeded sluggishly, requiring extended reaction times and affording the coupled material **129** in poor yield. In addition, purification of the reaction mixture was complicated by the presence of triphenylphosphine oxide, which could not be completely removed from the product by chromatography. This mixture could, however, be hydrolyzed and the triphenylphosphine oxide removed by extraction with ether.

Extension of this amidoalkylation reaction to phosphonomethyl-substituted (2-phenylethyl)carbamates **139** and **140** provided entry into the 6- and 7-(phosphonomethyl)tetrahydroisoquinoline derivatives **95** and **97** (Scheme III). Although the amidoalkylation reaction of **139** with glyoxylic acid gave a 6:1 ratio of regioisomeric products **141** and **143**,³⁸ Fischer esterification of this

(32) The isoquinoline **89** has a calculated log *P* (using version 3.54 of the CLOGP program from Daylight, Inc. of Pomona, CA) 1.4 log units higher than that of **1** (the contribution from the PO₃H₂ moiety was excluded from both calculations).

(33) Hirao, T.; Masunaga, T.; Oshiro, Y.; Agawa, T. A Novel Synthesis of Dialkyl Arenephosphonates. *Synthesis* 1981, 56-71.

(34) Chen, Q.; Yang, Z. Palladium-catalyzed Reaction of Phenyl Fluoroalkanesulfonates with Alkynes and Alkenes. *Tetrahedron Lett.* 1986, 1171-1174.

(35) Vorbruggen, H.; Kroklikiewicz, K. Trimethylsilyl as Leaving Group; III. A Simple One-Step Conversion of Aromatic Heterocyclic *N*-oxides to α -Cyano Aromatic *N*-Heterocycles. *Synthesis* 1983, 316-319.

(36) Ben-Ishai, D.; Satay, I.; Peled, N.; Goldshare, R. Intra vs Intermolecular Amidoalkylation of Aromatics. *Tetrahedron* 1987, 439-450.

(37) Grazi, C. O.; Corral, R. H.; Giaccio, H. Synthesis of Fused Heterocycles: 1,2,3,4-Tetrahydroisoquinolines and Ring Homologues via Sulphonamidomethylation. *J. Chem. Soc., Perkin Trans. 1* 1986, 1977-1982.

(38) The regioisomer ratios were determined by integration of the ¹H NMR spectra.

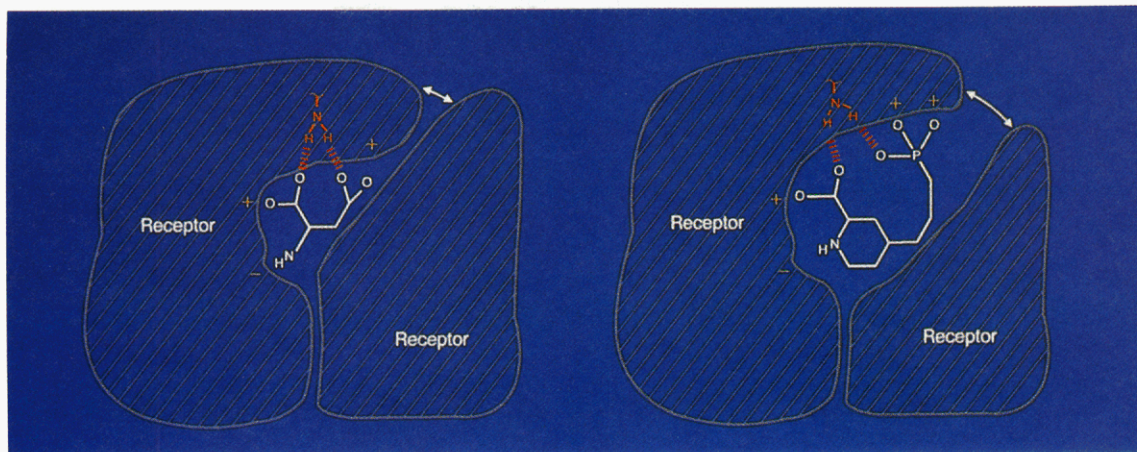


Figure 18. Hypothetical NMDA agonist (left, with L-ASP (5) bound) and antagonist (right, with CPP (1) bound) receptor sites. It is proposed that agonists and antagonists bind to the same receptor site off of one face (west and northwest), interacting with the same receptor moieties (a hypothetical receptor amine has been added as an illustration), but the larger antagonists bind to additional sites to the north and prevent a conformational change in the receptor that is responsible for agonist activity.

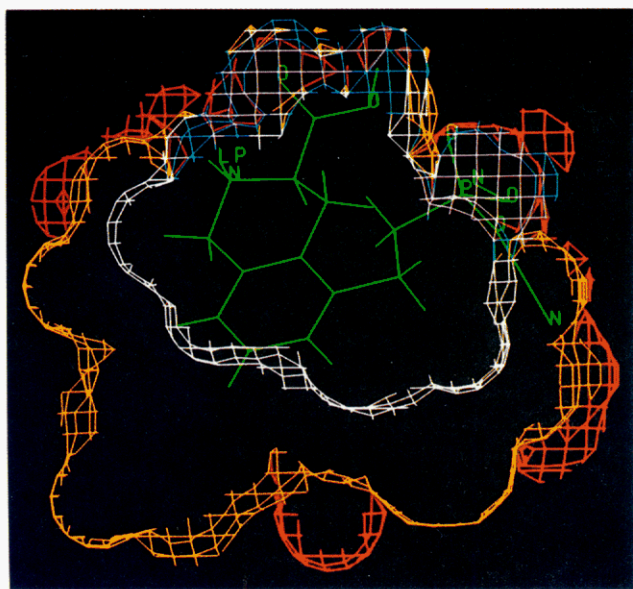
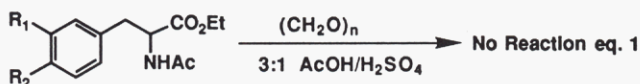


Figure 19. Fit of the designed isoquinoline 89 in the pharmacophore model. Surfaces correspond to receptor tolerated and excluded volumes; see Figure 15.

mixture unexpectedly provided 144 in greater than 95% isomeric purity,^{38,39} perhaps due to a neighboring group interaction between the carboxylate and phosphonate functionalities in 143.

Efforts toward the preparation of (phosphonoalkyl)-3-carboxytetrahydroisoquinolines also relied on amidoalkylation technology. Initial attempts to effect the cyclization of *N*-acetyl-4-bromophenylalanine (147) with formaldehyde failed (eq 1); subsequent replacement of the



147 R₁=H, R₂=Br

148 R₁=CH₂PO₃Et₂, R₂=H

p-bromo substituent with a *m*-phosphonomethyl group (148) failed as well. However, transformation of the ace-

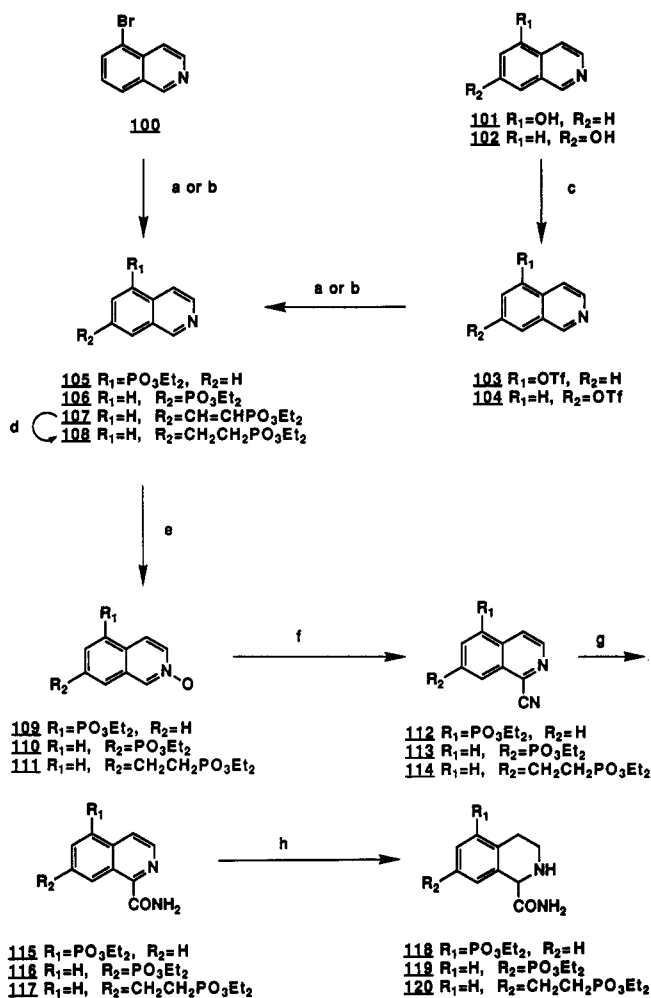
tamidomalonnate derivatives 149 and 150 to the carbamoyl esters 154 and 156, followed by treatment with formaldehyde, provided the required methyl 5- and 7-bromotetrahydroisoquinoline-3-carboxylate intermediates 157 and 158 in moderate yield (Scheme IV). Elaboration to the target compounds 87, 89, 91, and 93 was accomplished using standard conditions. Subsequently, it was discovered that modification of the acetamidomalonnate adducts was not necessary, since the corresponding diethyl *N*-(ethoxycarbonyl)malonnates 169–172 also underwent facile amidocyclization to afford the target tetrahydroisoquinolines directly (Scheme V). As in previous examples, it proved possible to simultaneously deprotect and decarboxylate these compounds in refluxing 6 N HCl. In addition to the phosphonomethyl derivatives 88, 90, and 92, the propanoic acid derivative 99 was also prepared utilizing a palladium(II) coupling of the 5-bromo derivative 173 with ethyl acrylate, followed by hydrogenation and hydrolysis.

Structure–Activity Relationships

The [³H]CPP receptor binding affinities for the entire set of 1- and 3-carboxytetrahydroisoquinolines, together with quinoline 21, are shown in Table IX. As mentioned above, an initial set of these compounds was prepared to investigate the effect of further constraining the conformational flexibility of a previously reported¹¹ series of phenyl-spaced phosphonoalkanoic acids while retaining the aryl moiety to maintain increased lipophilicity relative to the alicyclic antagonists AP5 (3) and AP7 (4). Therefore, it is interesting to compare the SARs of the two series, in light of the antagonist pharmacophore model described above.

For the 1-carboxyisoquinolines 96–98, which correspond to the meta,0,*x*-substituted phosphonoalkylphenylglycines, roughly comparable receptor binding was observed (Table IX). Of interest are the affinities of 94 and 96, which represent locked syn and anti forms of the meta,0,0 analogue. Consistent with the pharmacophore model, a syn orientation of the two acidic functionalities is preferred. The reduced potency of 95 over the para,0,1 analogue can be explained by excluded volume occupation in reaching the primary receptor point and the fact that the secondary receptor point could not be adequately reached due to steric clashes with the phenyl ring. This is because the phenyl ring in the para,0,1 analogue could be rotated approximately 90° out of the plane of the amino acid portion to accommodate a folding of the side chain back to the

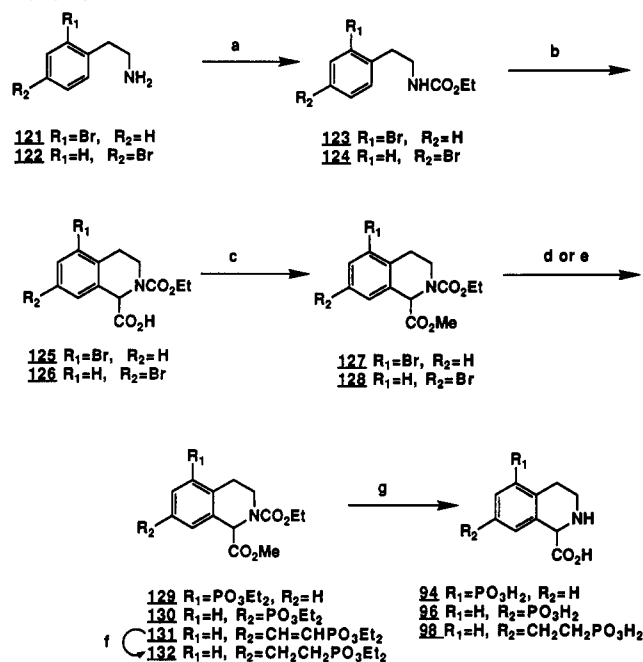
(39) The regiochemistry of the major product was established by a DNOE experiment.

Scheme I^a

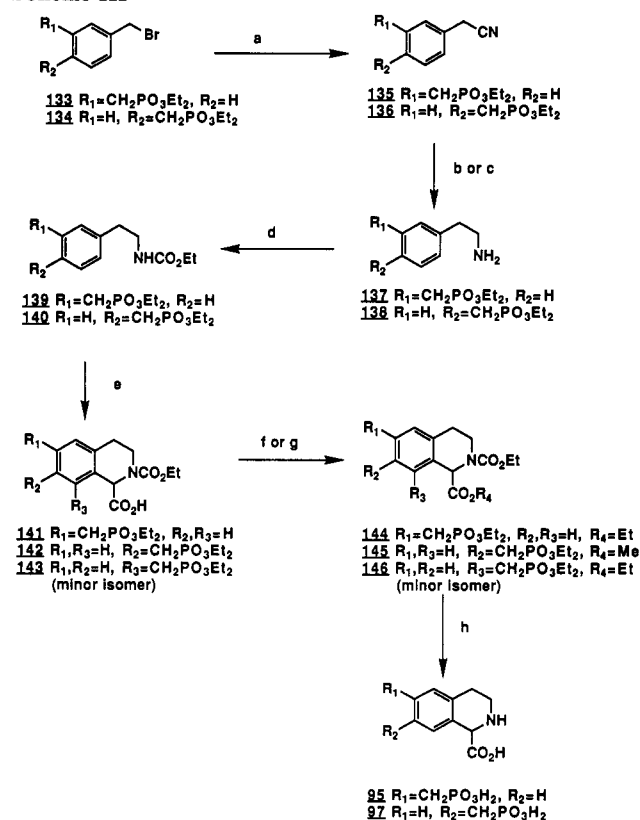
^a (a) (Ph₃P)₄Pd(0), HPO₃Et₂, Et₃N, toluene, 90–100 °C; (b) (Ph₃P)₂Pd(II)Cl₂, CH₂CHPO₃Et₂, Et₃N, DMF, 90 °C; (c) *N*-phenyltrifluoromethanesulfonamide, (*i*-Pr)₂Et₃N, MeOH, 25 °C; (d) H₂, 5% Pd/C, EtOH; (e) *m*-CPBA, CH₂Cl₂, 0 °C; (f) Me₃SiCN, Et₃N, 90 °C; (g) H₂SO₄, 90 °C; (h) H₂, 10% Pd/C, MeOH; (i) 6 N HCl, reflux.

receptor interaction points (for an example of this, see 20 in Figure 11), while the conformationally restricted analogue 95 is prevented from doing so. The progressive loss in affinity on extending side-chain length in the 96–98 series reflects both a difficulty in reaching the distal acidic binding sites and increased excluded volume occupation for the higher homologues.

Similar to the *para*,1,*x* series of (phosphonoalkyl)phenyl glycines, the 7-substituted 3-carboxytetrahydroisoquinolines 91–93 were devoid of significant receptor affinity. These compounds were generally too large to fit the receptor pocket and projected their distal acidic groups away from the primary and secondary receptor sites (they are *anti* substituted; see above). The *meta*,1,1 phosphonoalkyl alanine and its locked analogue 90 displayed

Scheme II^a

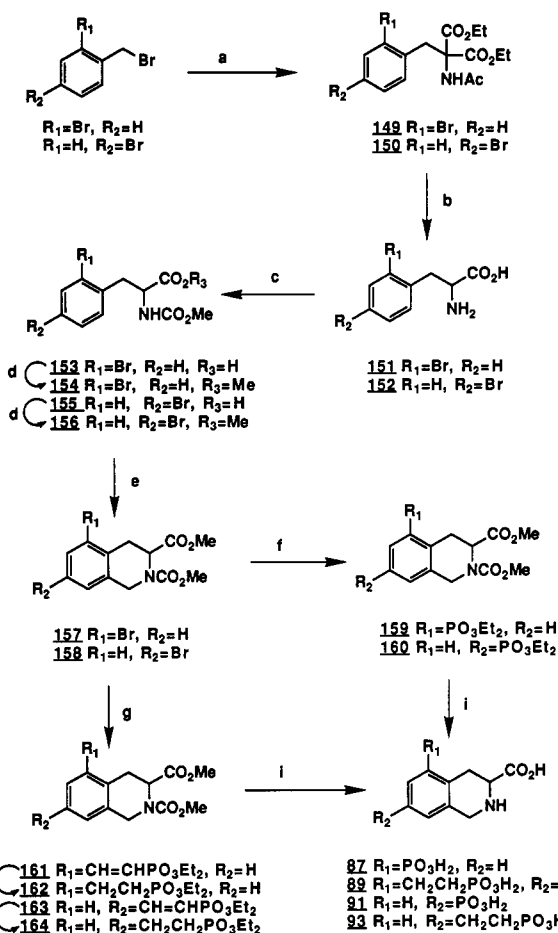
^a (a) ClCO₂Et, Et₃N, CH₂Cl₂, 0 °C; (b) OHCCO₂H, 3:1 AcOH/H₂SO₄ (v/v), 25 °C; (c) CH₂N₂, THF; (d) (Ph₃P)₄Pd(0), HPO₃Et₂, Et₃N, toluene, 90–100 °C; (e) (Ph₃P)₂Pd(II)Cl₂, CH₂CHPO₃Et₂, Et₃N, DMF, 90 °C; (f) H₂, 5% Pd/C, MeOH; (g) 6 N HCl, reflux.

Scheme III^a

^a (a) KCN, NaI, 3:1 acetone/H₂O; (b) H₂, Ni(Raney), MeOH/NH₃; (c) NaBH₄, CF₃CO₂H, THF; (d) ClCO₂Et, Et₃N, CH₂Cl₂; (e) OHCCO₂H, 3:1 AcOH/H₂SO₄ (v/v), 25 °C; (f) CH₂N₂, THF; (g) EtOH, H₂SO₄; (h) 6 N HCl, reflux.

equivalent receptor affinities, both being able to reach the distal acidic binding sites equally well.

Constraining the *ortho*,1,*x* series of (phosphonoalkyl)phenyl alanines to give the corresponding isoquinolines

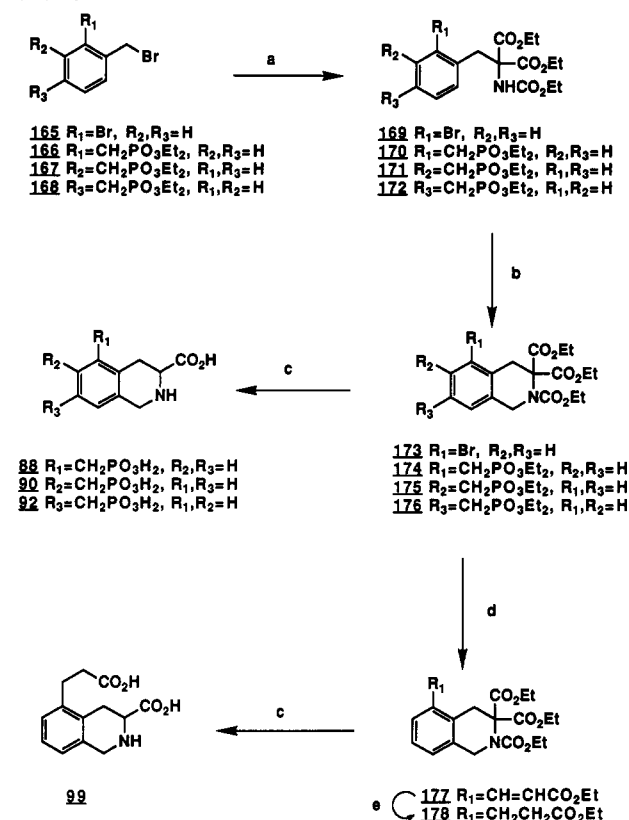
Scheme IV^a

^a (a) Diethyl acetamidomalonate, NaOEt, EtOH; (b) 6 N HCl, reflux; (c) ClCO₂Me, 1 N NaOH; (d) CH₂N₂, THF; (e) (CH₂O)_n, 3:1 AcOH/H₂SO (v/v); (f) (Ph₃P)₄Pd(0), HPO₃Et₂, Et₃N, toluene, 90–110 °C; (g) (Ph₃P)₂Pd(II)Cl₂, CH₂CHPO₃Et₂, Et₃N, DMF, 90 °C; (h) H₂, 5% Pd/C; MeOH; (i) 6 N HCl, reflux.

87–89 afforded the most dramatic increases in affinity. As predicted from the pharmacophore model, locking the phenyl ring in an orientation that projected the distal acidic group directly toward the primary and secondary binding sites as well as removing one *o*-phenyl hydrogen resulted in an increase in affinity from 60.9 to 0.27 μM for 89, and from >100 μM to 0.82 μM for 87. The fit of 89 in the pharmacophore model is shown in Figure 19.

In addition to their relationship with the phenyl-spaced phosphonoalkanoic acids, the isoquinolines described herein also represent conformationally restricted, lipophilic analogues of the antagonists CPP (1), CGS19755 (2), AP5 (3), and AP7 (4). In 87, the direct analogue of 2 and 3, the phosphonate is directly attached to the aromatic ring, and results in an 18-fold decrease in potency over 2. However, this substitution (as well as any substitution α to the distal acid) is known²⁶ to reduce affinity and could be due to rotational restrictions on the distal acid, simple volume intolerance in this area, or adverse electronic effects on the acid. In any event, this can also be used to rationalize, at least in part, the reduced affinities displayed by 91, 94, and especially 96. The higher homologue 89, which does not contain any substitution α to the distal acid or any significant excluded volume, is only 2.4-fold less potent than its comparable analogue CPP (1) and is ca. 4-fold more potent than the corresponding alicyclic analogue, AP7 (4).

Also of note is the periodicity in IC₅₀ values exhibited by the homologous series 87–88–89, which, although

Scheme V^a


^a (a) Diethyl *N*-carbethoxymalonate, EtONa, EtOH; (b) (CH₂)_n, 3:1 AcOH/H₂SO₄ (v/v); (c) 6 N HCl, reflux; (d) CH₂CHCO₂Et, (Ph₃P)₂Pd(II)Cl₂, Et₃N, DMF, 90 °C; (e) H₂, 5% Pd/C, EtOH.

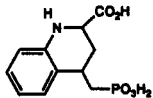
mutated,⁴⁰ parallels the observed periodicity in the AP5–6–7 series (Table VI). Consistent with literature reports² and our own observations,^{10a} replacing the distal phosphonic acid of 89 with a carboxylate to give 99 resulted in reduced affinity (Table IX). Quinoline 21, while retaining significant affinity for the receptor, was 16-fold less potent than CGS 19755 (2), presumably due to excluded volume occupation by (a portion of) the benzo ring, when optimally oriented for binding.

Conclusions

The NMDA agonist and competitive antagonist pharmacophore models described in this communication have proven to be valuable in the rationalization of observed receptor binding activity and in the design of novel antagonists. Although agonists and competitive antagonists likely bind to the same recognition site, there has been evidence to suggest that antagonists might bind to a separate receptor.⁴ In addition, the binding of 1 and 2, both reference standards for competitive inhibition, have been shown to be differentially regulated by the coagonist glycine,⁴¹ suggesting the possibility of different binding modes

- (40) Although the difference in affinity between 87 and 88 is outside the standard errors of the IC₅₀ determinations, this difference is marginal when compared to the variation in affinity between the analogous compounds AP5 and AP6, and 82 and 83 (Table VI). However, we felt that the reduced affinity of 87 was due to a direct attachment of the PO₃H₂ moiety to an aryl ring, a substitution known²⁶ to reduce affinity, and not due to a poor fit to the receptor site points or the projection of the third (ketonic) oxygen.
- (41) Kaplita, P. V.; Ferkany, J. W. Evidence for Direct Interactions Between the NMDA and Glycine Recognition Sites in Brain. *Eur. J. Pharmacol.* 1990, 188, 175–179.

Table IX. Comparison of 1- and 3-Carboxytetrahydroisoquinoline Alkylphosphonates with Their Corresponding Nonfused Phenyl-Spaced Phosphonoalkanoic Acids


no.	R ₁	R ₂	R ₃	IC ₅₀ , ^a μM (% inhibit at 10 ⁻⁴ M)	nonfused equivalent, ^b subst, n, m	IC ₅₀ , ^{a,b} (μM) (% inhibit at 10 ⁻⁴ M)	comments
87	H	CO ₂ H	5-PO ₃ H ₂	0.82 ± 0.19	ortho, 1, 0	(3%)	
88	H	CO ₂ H	5-CH ₂ PO ₃ H ₂	1.95 ± 0.60	ortho, 1, 1	8.4	c
89	H	CO ₂ H	5-CH ₂ CH ₂ PO ₃ H ₂	0.27 ± 0.05 ^d	ortho, 1, 2	60.9	e
90	H	CO ₂ H	6-CH ₂ PO ₃ H ₂	4.08 ^f	meta, 1, 1	3.3	g
91	H	CO ₂ H	7-PO ₃ H ₂	(0%)	para, 1, 0	(10%)	
92	H	CO ₂ H	7-CH ₂ PO ₃ H ₂	(0%)	para, 1, 1	(1%)	
93	H	CO ₂ H	7-CH ₂ CH ₂ PO ₃ H ₂	(0%)	para, 1, 2	—	
94	CO ₂ H	H	5-PO ₃ H ₂	(0%)	meta, 0, 0	17.4	h
95	CO ₂ H	H	6-CH ₂ PO ₃ H ₂	61.0 ± 12.8	para, 0, 1	1.0	
96	CO ₂ H	H	7-PO ₃ H ₂	1.9 ± 0.79	meta, 0, 0	17.4	h
97	CO ₂ H	H	7-CH ₂ PO ₃ H ₂	37.2 ± 6.8	meta, 0, 1	9.3	
98	CO ₂ H	H	7-CH ₂ CH ₂ PO ₃ H ₂	(22%) ⁱ	meta, 0, 2	(35%)	
99	H	CO ₂ H	5-CH ₂ CH ₂ CO ₂ H	14.5 ± 4.9			
21				0.85			

^a For displacement of [³H]CPP from rat brain membranes ● the standard error of the mean (SEM), for those compounds with IC₅₀ values. Unless otherwise indicated, n = 6. See the Experimental Section. ^b Reference 11. ^c Phenylalanine derivative data not previously published. ^d n = 9. ^e Phenylalanine derivative corresponds to NPC451 (64, Table V). ^f n = 3. ^g Cyclization to the isoquinoline 90 could have afforded as a minor product 3-carboxy-8-(phosphonomethyl)tetrahydroisoquinoline. None was apparent from the NMR. This compound would have been expected to have no affinity for the receptor. ^h The meta, 0, 0 phenylglycine is equivalent to the isoquinolines 94 and 96. ⁱ n = 2.

at the receptor. However, the fact that we were able to derive a consistent superposition for a wide variety of agonists and antagonists argues for the presence of at least one site within the NMDA receptor complex that is capable of accommodating these ligands.

It is likely that the CO₂H and PO₃H₂ groups within these agonists and antagonists exist as mono- and dianions, respectively, at physiological pH. Although the modeling calculations could have been run on the ionized species, we felt that doing so would introduce more uncertainties than it would remove. Specifically, one then has to choose which charges to employ, worry about the parameterization of charged species within the force fields, decide how to include solvent or other counterions such as salts in the

calculations, etc. The resulting geometries from such calculations will then undoubtedly be dependent on the conditions employed, which may or may not reflect the situation at the active site of the NMDA receptor complex. Therefore, we chose not to employ charges in the minimizations. Although the resulting geometries may be compromised by such simplifications, the correct predictions of activities for novel antagonists argue in favor of the validity of these models.

While the analogues reported herein have somewhat reduced affinity relative to known standards, the correct predictions of potency demonstrate the utility of molecular modeling in the design of novel, more lipophilic antagonists. The relatively low receptor affinities of the predicted compounds may be due in part to the extremely tight volume tolerances surrounding the inhibitors, the difficulty of the rigid isoquinolines to gain access to the recognition site, or in part because the model was derived from small molecules. More accurate predictions will have to wait for a precise knowledge of the three dimensional structure of the receptor itself. Reports on the use of these models in the design of additional analogues will be forthcoming from our laboratories.

- (42) Lehman, J.; Schneider, J. A.; Williams, M. Excitatory Amino Acids and Mammalian CNS Function. *Annu. Rep. Med. Chem.* 1987, 22, 31.
- (43) Watkins, J. C. Pharmacology of Excitatory Amino Acid Receptors in *Glutamate: Transmitter in the Central Nervous System*; Roberts, P. J., Storm-Mathisen, J., Johnson, G. A. R., Eds.; John Wiley and Sons Ltd.: New York, 1981; pp 1-24.
- (44) Davies, J.; Evans, R. H.; Francis, A. A.; Jones, A. W.; Smith, D. A.; Watkins, J. C. Conformational Aspects of the Actions of Some Piperidine Dicarboxylic Acids at Excitatory Amino Acid Receptors in the Mammalian and Amphibian Spinal Cord. *Neurochem. Res.* 1982, 7, 1119-1133.
- (45) Leach, M. J.; Marden, C. M.; Canning, H. M. (±)-Cis-2,3-piperidine Dicarboxylic Acid is a Partial N-methyl-D-aspartate Agonist in the In Vitro Rat Cerebellar cGMP Model. *Eur. J. Pharm.* 1986, 121, 173-179.
- (46) Wheatley, P. L.; Collins, K. J. Quantitative Studies of N-methyl-D-aspartate, 2-amino-5-phosphonovalerate and cis-2,3-piperidine Dicarboxylate Interactions on the Neonatal Rat Spinal Cord In Vitro. *Eur. J. Pharm.* 1986, 121, 257-263.
- (47) Curry, K.; Peet, M. J.; Magnuson, D. S. K.; McLennan, H. Synthesis, Resolution, and Absolute Configuration of the Isomers of the Neuronal Excitant 1-amino-1,3-cyclopentanedicarboxylic Acid. *J. Med. Chem.* 1988, 31, 864-867.

- (48) Krosgaard-Larsen, P.; Honore, T.; Hansen, J. J.; Curtis, D. R.; Lodge, D. New Class of Glutamate Agonist Structurally Related to Ibotenic Acid. *Nature* 1980, 284, 64-66.
- (49) Krosgaard-Larsen, P. GABA and Glutamic Acid Agonists of Pharmacological Interest in *Fast and Slow Chemical Signalling in the Nervous System*; Iverson, L. L., Goodman, E. G., Eds.; Oxford University Press: London, 1986; pp 75-89.
- (50) Hays, S. J.; Bigge, C. F.; Drummond, J. T.; Johnson, G.; Brahe, L. J.; Coughenour, L. L.; Robichaud, L. J. Novel Heteroaryl-Spaced APV and APH Analogues as Ligands for the NMDA Receptor. *Neurochem. Int.* 1990, 16 (1), 43.
- (51) Hutchinson, A. J.; Shaw, K. R.; Schneider, J. A. Eur. Patent 0 203 891 A2, 1986.

Experimental Section

Melting points were determined on a Thomas-Hoover capillary melting point apparatus and are uncorrected. IR spectra were obtained on a Nicolet MX-1 FT spectrometer. ^1H NMR spectra were obtained on an IBM WP100SY NMR spectrometer (100 MHz), Varian XL200 NMR spectrometer (200 MHz), Varian XL300 NMR spectrometer (300 MHz), or a Bruker WM 250 NMR spectrometer (250 MHz) and were consistent with proposed structures. The peaks are described in parts per million (ppm) downfield from tetramethylsilane (internal standard). Coupling constants (J) are reported in hertz. Mass spectra were obtained on Finnegan 4500 or VG Analytical 7070E/HF spectrometers. Where analyses are indicated by element symbols, the results are within 0.4% of the theoretical values; values outside these limits are indicated. TLC was carried out using 0.25-mm silica gel F254 (E. Merck) glass plates. Column chromatography used E. Merck silica gel (230–400 mesh).

Chemistry. 5-[[Trifluoromethylsulfonyl]oxy]isoquinoline (103). A solution of 5-hydroxyisoquinoline (20.0 g, 0.138 mol) and diisopropylethylamine (23 mL) in methanol (300 mL) was cooled to 0 °C and *N*-phenyltrifluoromethanesulfonimide (60 g, 168 mmol) was added. The resulting solution was stirred at room temperature for 18 h and concentrated. The residue was purified by silica gel chromatography (3:2 heptane/EtOAc) to give a tan solid (26.3 g, 69%).

7-[[Trifluoromethylsulfonyl]oxy]isoquinoline (104). A solution of 7-hydroxyisoquinoline⁶² (9.75 g, 67.2 mmol) gave 104 as a colorless oil (14.4 g, 77%) by the method described for the preparation of 103.

Diethyl 5-Isoquinolinylphosphonate (105). A solution of 5-bromoisoquinoline (100)⁶³ (5.0 g, 24 mmol), diethyl phosphite (3.4 mL, 26 mmol), and tetrakis(triphenylphosphine)palladium(0) (1.4 g, 1.2 mmol) in 25 mL of toluene was heated at 50 °C under a N_2 atmosphere for 3 h and then at 90 °C for an additional 15

h. The reaction mixture was cooled to room temperature and treated with toluene. After filtration and concentration, the residue was purified by silica gel chromatography (EtOAc) to give 105 as a yellow oil (5.04 g, 79%): ^1H NMR (100 MHz, CDCl_3) δ 9.34 (d, 1 H, $J = 1.7$), 8.69 (d, 1 H, $J = 6.6$), 8.60–8.13 (m, 3 H), 7.82–7.60 (m, 1 H), 4.40–4.00 (m, 4 H), 1.37 (t, 6 H, $J = 7.0$); MS (EI) m/e 265 (M^+). Anal. ($\text{C}_{13}\text{H}_{16}\text{NPO}_3$) C, H, N.

Diethyl 7-Isoquinolinylphosphonate (106). A solution of 104 (10.5 g, 37.8 mmol), *N*-methylmorpholine (5.9 mL, 49.3 mmol), diethyl phosphite (5.9 mL, 45.2 mmol), and tetrakis(triphenylphosphine)palladium(0) (1.31 g, 1.13 mmol) in 105 mL of CH_3CN was heated at 70 °C for 24 h. The reaction was concentrated and purified by silica gel chromatography (EtOAc) to give 106 as a gold oil (12.55 g): ^1H NMR (200 MHz, CDCl_3) δ 9.54 (s, 1 H), 8.70 (s, 1 H), 8.62 (d, 1 H, $J = 9.9$), 8.13 (dd, 1 H, $J = 8.6, 3.8$), 8.02–7.92 (m, 2 H), 4.17–4.01 (m, 4 H), 1.26 (t, 6 H, $J = 7.1$); MS (EI) m/e 265 (M^+).

Diethyl [2-(7-Isoquinolinyl)ethenyl]phosphonate (107). A solution of 104 (14.4 g, 51.9 mmol), diethyl vinylphosphonate (11.5 mL, 74.8 mmol), and bis(triphenylphosphine)palladium(II) dichloride (1.1 g, 1.57 mmol) in 100 mL of DMF and 29 mL of triethylamine was heated at 90 °C for 24 h. The reaction mixture was concentrated and the residue purified by silica gel chromatography (9:1 EtOAc/EtOH) to give 107 as a red oil (19.9 g): ^1H NMR (100 MHz, CDCl_3) δ 9.20 (s, 1 H), 8.13 (d, 1 H, $J = 4$), 8.66 (d, 2 H, $J = 5$), 7.80 (s, 1 H), 7.62 (d, 2 H, $J = 4$), 6.42 (t, 1 H, $J = 11$), 4.10 (m, 4 H), 1.38 (t, 6 H, $J = 5$).

Diethyl [2-(7-Isoquinolinyl)ethyl]phosphonate (108). A solution of 107 (18.0 g, 61.9 mmol) in 100 mL of EtOH was hydrogenated at 52 psi over 5% Pd/C (2.0 g) for 71 h. Because TLC showed the reaction to be incomplete, the mixture was filtered through Celite and concentrated, and the resulting oil was dissolved in 100 mL of EtOH and further hydrogenated at 52 psi over 10% Pd/C (3.0 g) for 5.6 h. The reaction mixture was filtered through Celite and concentrated to give 108 as a yellow oil (11.5 g, 63%): ^1H NMR (100 MHz, CDCl_3) δ 9.26 (s, 1 H), 8.44 (d, 1 H, $J = 5.0$), 7.97–7.68 (m, 4 H), 4.17–3.77 (m, 4 H), 3.13–2.82 (m, 2 H), 2.33–1.96 (m, 2 H), 1.20 (t, 6 H, $J = 7.1$).

Diethyl 5-Isoquinolinylphosphonate *N*-Oxide (109). A solution of 105 (4.30 g, 16.2 mmol) in 100 mL of CH_2Cl_2 was cooled to 0 °C and treated with *m*-chloroperoxybenzoic acid (MCPBA) (3.0 g, 17.4 mmol). After 30 min, additional MCPBA (1.6 g, 9.27 mmol) was added. The reaction mixture was stirred for 18 h at room temperature and treated with 20% aqueous K_2CO_3 (100 mL). The organic phase was collected, dried (Na_2SO_4), and concentrated to give 109 as a gold oil (4.57 g, 100%). This material was not characterized, but used directly in the preparation of 112.

Diethyl 7-Isoquinolinylphosphonate *N*-Oxide (110). Compound 106 (11.83 g, 35.7 mmol) gave 110 as an oil (6.61 g, 66%) by the method described for the preparation of 109. This material was not characterized, but used directly in the preparation of 113.

Diethyl [2-(7-Isoquinolinyl)ethyl]phosphonate *N*-Oxide (111). Compound 108 (11.0 g, 37.0 mmol) gave 111 as an oil (8.49 g, 74%) by the method described for the preparation of 109. This material was not characterized, but used directly in the preparation of 114.

Diethyl (1-Cyano-5-isoquinolinyl)phosphonate (112). A suspension of 109 (4.00 g, 14.2 mmol) in trimethylsilyl cyanide (12.0 mL, 89.9 mmol) and triethylamine (5.6 mL, 40.2 mmol) was heated at 90 °C for 2 h. The resulting dark solution was poured into a cold saturated aqueous solution of NaHCO_3 , stirred for 1 h, and extracted with CH_2Cl_2 . The extract was dried (Na_2SO_4) and concentrated and the residue purified by chromatography (EtOAc) to give 112 as an orange solid (2.71 g, 66%): ^1H NMR (100 MHz, CDCl_3) δ 8.83–8.30 (m, 4 H), 7.97–7.77 (m, 1 H), 4.40–4.00 (m, 4 H), 1.29 (t, 6 H, $J = 7.0$). Anal. ($\text{C}_{14}\text{H}_{15}\text{N}_2\text{O}_3\text{P}$) C, H, N.

Diethyl (1-Cyano-7-isoquinolinyl)phosphonate (113). Compound 110 (6.6 g, 23.5 mmol) gave 113 as an orange solid (3.00 g, 44%) by the method described for the preparation of 112: mp 101–106 °C; ^1H NMR (200 MHz, CDCl_3) δ 8.88–8.76 (m, 2 H), 8.24–7.94 (m, 3 H), 4.33–4.15 (m, 4 H), 1.39 (t, 6 H, $J = 7.2$). Anal. ($\text{C}_{14}\text{H}_{15}\text{N}_2\text{O}_3\text{P}$) C, H, N: calcd, 9.65; found, 9.05.

Diethyl [2-(1-Cyano-7-isoquinolinyl)ethyl]phosphonate (114). Compound 111 (8.49 g, 28.0 mmol) gave 114 as an oil (3.23 g, 36%) by the method described for the preparation of 112: ^1H

- (52) (a) Bigge, C. F.; Johnson, G.; Marcoux, F. W.; Probert, A. W.; Coughenour, L. L.; Brahce, L. J. *N*-(Phosphonoalkyl) and -Aryl Substituted- α -Amino Acids as Competitive Inhibitors of the NMDA Receptor. *Soc. Neurosci. Abstr.* 1989, 15, 463. (b) Bigge, C. F.; Johnson, G.; Ortwine, D. F.; Drummond, J. T.; Retz, D. M.; Brahce, L. J.; Coughenour, L. L.; Marcoux, F. W.; Probert, A. W., Jr. Exploration of *N*-Phosphonoalkyl, *N*-Phosphonoalkenyl, and *N*-(Phosphonoalkyl)phenyl-Spaced α -Amino Acids as Competitive *N*-Methyl-D-aspartic Acid Antagonists. *J. Med. Chem.*, companion paper in this issue.
- (53) (a) Watkins, J. C.; Jones, A. W. Eur. Patent 0 159 889 A2, 1985. (b) Hays, S. J. Unpublished results.
- (54) Jones, A. W.; Smith, D. A. S.; Watkins, J. C. Structure-Activity Relations of Dipeptide Antagonists of Excitatory Amino Acids. *Neuroscience* 1984, 13, 573–581.
- (55) Rzeszotarski, W. J.; Hudkins, R. L.; Guzewska, M. E. United States Patent 4,657,899.
- (56) (a) Angst, C.; Brundish, D. E.; Grey, J. G.; Fagg, G. E. European Patent 233,154. (b) Fagg, G. E.; Olpe, H.-R.; Bittiger, H.; Schmutz, M.; Angst, C.; Brundish, D.; Allgeier, H.; Hecken-dorn, R.; Dingwall, J. G. CGP 37849 and CGP 39551: Potent and Selective Competitive NMDA Receptor Antagonists with Oral Activity. *Soc. Neurosci. Abstr.* 1988, 14, 941, part 2. (c) Fagg, G. E.; Olpe, H. R.; Pozza, M. F.; Baud, J.; Steinmann, M.; Schmutz, M.; Portet, C.; Baumann, P.; Thedinga, K. CGP 37849 and CGP 39551: Novel and Potent Competitive *N*-methyl-D-aspartate Receptor Antagonists with Oral Activity. *Br. J. Pharmacol.* 1990, 99, 791–797.
- (57) Wedler, F. C.; Farrington, G. K.; Kumar, A.; Biggi, C. F.; Ortwine, D. F.; Johnson, G. 3-[(Phosphonomethyl)sulfinyl]-D,L-Alanine, A Potent *N*-methyl-D-aspartate Receptor Antagonist. *Life Sci. Adv. Neurochem.* 1992, in press. (b) Muller, W.; Herrling, P. L. GB(A) 2 156 818, 1985.
- (58) Hutchinson, A. J. Personal communication.
- (59) Herrling, P. L.; Muller, W. GB(A) 2 198 134, 1988.
- (60) Bigge, C. F. Unpublished results.
- (61) Vazquez, M. L. Personal communication.
- (62) Woodward, R. B.; Doering, W. D. The Total Synthesis of Quinine. *J. Am. Chem. Soc.* 1945, 67, 860–874.
- (63) Gordon, M.; Pearson, D. E. The Swamping Catalyst Effect. VI. The Halogenation of Isoquinoline and Quinoline. *J. Org. Chem.* 1964, 29, 329–332.

NMR (100 MHz, CDCl_3) δ 8.50 (d, 1 H, $J = 6.7$), 8.00 (s, 1 H), 7.87–7.48 (m, 3 H), 4.22–3.84 (m, 4 H), 3.27–2.92 (m, 2 H), 2.31–1.88 (m, 2 H), 1.24 (t, 6 H, $J = 7.1$).

Diethyl [1-(Aminocarbonyl)-5-isoquinolinyl]phosphonate (115). A suspension of 112 (2.4 g, 8.53 mmol) in 15 mL of concentrated H_2SO_4 was heated at 90 °C for 10 min. The resulting solution was cooled to 0 °C, poured into a solution of Na_2CO_3 , and extracted into CH_2Cl_2 . The organic phase was dried (Na_2SO_4), filtered, and concentrated to give a tan solid (1.66 g). The solid was suspended in $i\text{-Pr}_2\text{O}$, collected, and dried to give 115 (1.32 g, 50%): mp 128–129 °C; IR (KBr) 1681 cm^{-1} ; ^1H NMR (100 MHz, CDCl_3) δ 9.83 (d, 1 H, $J = 9.3$), 8.67–8.32 (m, 3 H), 8.14–7.88 (bs, 1 H), 7.86–7.63 (m, 1 H), 5.95–5.67 (bs, 1 H), 4.39–3.98 (m, 4 H), 1.32 (t, 6 H, $J = 7.0$); MS (EI) m/e 308 (M^+). Anal. ($\text{C}_{14}\text{H}_{17}\text{N}_2\text{O}_4\text{P}$) C, H, N.

Diethyl [1-(Aminocarbonyl)-7-isoquinolinyl]phosphonate (116). Compound 113 (2.85 g, 9.82 mmol) gave 116 as a tan solid (1.64 g, 54%) by the method described for the preparation of 115: mp 125–127 °C; IR (KBr) 1686 cm^{-1} ; ^1H NMR (100 MHz, DMSO) δ 9.43 (d, 1 H, $J = 16.6$), 8.67 (d, 1 H, $J = 5.6$), 8.46–7.80 (m, 5 H), 4.23–3.93 (m, 4 H), 1.30 (t, 6 H, $J = 7.0$); MS (EI) m/e 308 (M^+). Anal. ($\text{C}_{14}\text{H}_{17}\text{N}_2\text{O}_4\text{P}$) C, H, N.

Diethyl [2-[1-(Aminocarbonyl)-7-isoquinolinyl]ethyl]phosphonate (117). Compound 114 (3.18 g, 9.99 mmol) gave crude 117 (2.71 g) as a tan solid by the method described for the preparation of 115. Recrystallization from THF/ $i\text{-Pr}_2\text{O}$ provided 117 as a gold solid (2.33 g, 69%): mp 142–144 °C; IR (film) 1682 cm^{-1} ; ^1H NMR (200 MHz, DMSO) δ 8.77 (s, 1 H), 8.46 (d, 1 H, $J = 5.5$), 8.19 (bs, 1 H), 7.98–7.93 (m, 2 H), 7.77–7.72 (m, 2 H), 4.02–3.93 (m, 4 H), 2.99–2.93 (m, 2 H), 2.18–2.07 (m, 2 H), 1.19 (t, 6 H, $J = 7.0$); MS (EI) m/e 336 (M^+). Anal. ($\text{C}_{16}\text{N}_2\text{N}_2\text{O}_4\text{P}$) C, H, N.

Diethyl [1-(Aminocarbonyl)-1,2,3,4-tetrahydro-5-isoquinolinyl]phosphonate (118). A solution of 115 (1.15 g, 3.73 mmol) in 100 mL of MeOH was hydrogenated at 52 psi over 10% Pd/C (1.0 g) for 4.8 h. The reaction mixture was concentrated and the residue was purified by chromatography (EtOAc) to give 118 as an oil (0.91 g, 78%).

Diethyl [1-(Aminocarbonyl)-1,2,3,4-tetrahydro-7-isoquinolinyl]phosphonate (119). Compound 116 (1.51 g, 4.9 mmol) gave 119 as a pale gold oil (1.56 g) by the method described for the preparation of 118. This material was used without further purification in the preparation of 96.

Diethyl [2-[1-(Aminocarbonyl)-1,2,3,4-tetrahydro-7-isoquinolinyl]ethyl]phosphonate (120). Compound 117 (2.02 g, 6.0 mmol) gave 120 as an oil (1.40 g, 68%) by the method described for the preparation of 118.

Ethyl [2-(4-Bromophenyl)ethyl]carbamate (124). A solution of 4-bromophenethylamine (122) (10.0 g, 50 mmol) and triethylamine (5.3 g, 52.5 mmol) in 200 mL of CH_2Cl_2 was cooled to 0 °C and treated with ethyl chloroformate (5.69 g, 52.5 mmol). After stirring at 0 °C for 1 h, the mixture was washed with a saturated aqueous NaHCO_3 solution (50 mL), dried (MgSO_4), and concentrated to give 124 as an oil (12.3 g, 90%): ^1H NMR (250 MHz, CDCl_3) δ 7.43 (d, 2 H, $J = 8.3$), 7.07 (d, 2 H, $J = 8.3$), 4.65 (bs, 1 H), 4.10 (q, 2 H, $J = 7.2$), 3.09 (q, 2 H, $J = 7.4$), 2.77 (t, 2 H, $J = 6.8$), 1.23 (t, 3 H, $J = 7.2$).

Ethyl [2-(2-Bromophenyl)ethyl]carbamate (123). 2-Bromophenethylamine (121)⁶⁴ (3.60 g, 18.0 mmol) gave 123 as an oil (4.32 g, 88%) by the method described for the preparation of 124: ^1H NMR (250 MHz, CDCl_3) δ 7.55 (d, 2 H, $J = 7.8$), 7.31–7.05 (m, 2 H), 4.75 (bs, 1 H), 4.11 (q, 2 H, $J = 7.1$), 3.48–3.40 (m, 2 H), 2.96 (t, 2 H, $J = 7.1$), 1.23 (t, 3 H, $J = 7.1$).

7-Bromo-3,4-dihydro-1,2(1H)-isoquinolinedicarboxylic Acid, 2-Ethyl Ester (126). A solution of 124 (10.8 g, 39.8 mmol) in 3:1 glacial acetic acid/sulfuric acid (80 mL) was treated with glyoxylic acid monohydrate (4.07 g, 44.2 mmol). After stirring at room temperature for 24 h, the reaction mixture was poured onto ice (50 g), and the aqueous layer was extracted with CH_2Cl_2 (5 \times 50 mL). The organic extracts were combined, dried (Na_2SO_4), and concentrated to give 126 as a white solid (11.4 g, 87%): ^1H

NMR (250 MHz, CDCl_3) δ 7.67 (s, 1 H), 7.37 (dd, 1 H, $J = 8.2$, 2.0), 7.04 (d, 1 H, $J = 8.2$), 6.71 (bs, 1 H), 5.55 (d, 1 H, $J = 21.0$), 4.21 (q, 2 H, $J = 7.2$), 3.93–3.64 (m, 2 H), 2.92–2.77 (m, 2 H), 1.32–1.11 (m, 3 H).

5-Bromo-3,4-dihydro-1,2(1H)-isoquinolinedicarboxylic Acid, 2-Ethyl Ester (125). Compound 123 (1.91 g, 9.92 mmol) gave 125 as a viscous oil (2.22 g, 68%) by the method described for the preparation of 126: ^1H NMR (250 MHz, CDCl_3) δ 10.4 (bs, 1 H), 7.54–7.48 (m, 2 H), 7.11 (t, 1 H, $J = 7.9$), 5.61 (d, 1 H, $J = 29.1$), 4.26–3.86 (m, 3 H), 3.68–3.61 (m, 1 H), 2.95 (t, 2 H, $J = 5.9$), 1.33–1.20 (m, 3 H).

2-Ethyl 1-Methyl 7-Bromo-3,4-dihydro-1,2(1H)-isoquinolinedicarboxylate (128). A solution of 126 (8.35 g, 25.4 mmol) in 100 mL of THF was treated with an ethereal solution of diazomethane until a persistent yellow colored solution developed. The reaction mixture was concentrated, and the resulting solid was suspended in a 5:1 heptane/ $i\text{-Pr}_2\text{O}$ solution and filtered to give 128 as a white solid (4.09 g, 47%): mp 82–85 °C. Anal. ($\text{C}_{14}\text{H}_{16}\text{BrNO}_4$) C, H, N, Br. Concentration of the filtrate afforded additional product (4.08 g, 46%): IR (KBr) 1740, 1688 cm^{-1} ; ^1H NMR (250 MHz, CDCl_3) δ 7.64 (d, 1 H, $J = 1.7$), 7.36 (dd, 1 H, $J = 8.0$, 1.9), 7.04 (d, 1 H, $J = 8.0$), 5.56 (d, 1 H, $J = 23.6$), 4.20–4.03 (m, 2 H), 3.98–3.65 (m, 2 H), 3.74 (s, 3 H), 2.94–2.81 (m, 2 H), 1.33–1.23 (m, 3 H); MS (CI) m/e 343, 341 (MH^+).

2-Ethyl 1-Methyl 5-Bromo-3,4-dihydro-1,2(1H)-isoquinolinedicarboxylate (127). Compound 125 (2.00 g, 6.09 mmol) gave 127 as a white solid (1.44 g, 69%) by the method described for the preparation of 128: mp 50–53 °C; ^1H NMR (200 MHz, CDCl_3) δ 7.50 (t, 2 H, $J = 8.6$), 7.12 (t, 1 H, $J = 7.9$), 5.63 (d, 1 H, $J = 23.1$), 4.27–3.67 (m, 4 H), 3.74 (s, 3 H), 2.96 (t, 2 H, $J = 5.7$), 1.35–1.23 (m, 3 H); MS (CI) m/e 344, 342 ($\text{MH}^+ + 1$). Anal. ($\text{C}_{14}\text{H}_{16}\text{BrNO}_4$) C, H, N.

2-Ethyl 1-Methyl 7-(Diethoxyphosphinyl)-3,4-dihydro-1,2(1H)-isoquinolinedicarboxylate (130). A solution of 128 (4.00 g, 11.7 mmol), diethyl phosphite (1.69 g, 12.3 mmol), tetrakis(triphenylphosphine)palladium(0) (0.68 g, 0.6 mmol), and triethylamine (1.67 g, 16.5 mmol) in 50 mL of toluene was heated at reflux for 24 h. After cooling to room temperature, the reaction mixture was washed with H_2O (20 mL), and the aqueous phase was extracted with EtOAc (2 \times 30 mL). The combined organic extracts were dried (MgSO_4) and concentrated, and the residue was purified by chromatography (EtOAc) to give 130 as a yellow oil (2.69 g, 58%): IR (film) 1746, 1705 cm^{-1} ; ^1H NMR (250 MHz, CDCl_3) δ 7.92 (d, 1 H, $J = 13.8$), 7.79–7.63 (m, 1 H), 7.29–7.25 (m, 1 H), 5.65 (d, 1 H, $J = 23.3$), 4.26–3.75 (m, 8 H), 3.73 (s, 3 H), 3.04–2.87 (m, 2 H), 1.36–1.24 (m, 9 H); MS (EI) m/e 340 ($\text{M}^+ - 59$).

2-Ethyl 1-Methyl 5-(Diethoxyphosphinyl)-3,4-dihydro-1,2(1H)-isoquinolinedicarboxylate (129). A solution of 127 (1.96 g, 5.73 mmol), diethyl phosphite (1.07 g, 7.74 mmol), tetrakis(triphenylphosphine)palladium(0) (0.05 g), and triethylamine (1.08 g, 10.8 mmol) in 25 mL of toluene was heated at reflux for 48 h. Additional tetrakis(triphenylphosphine)palladium(0) (0.10 g) was added, and the reaction was heated an additional 48 h. The reaction mixture was worked up and product purified by the methods described for 130 to give 129 as an oil (1.06 g): IR (film) 1745, 1706 cm^{-1} ; ^1H NMR (250 MHz, CDCl_3) δ 7.92–7.82 (m, 1 H), 7.67 (d, 1 H, $J = 7.5$), 7.36–7.29 (m, 1 H), 5.62 (d, 1 H, $J = 26.4$), 4.28–4.09 (m, 6 H), 3.85–3.77 (m, 2 H), 3.72 (s, 3 H), 3.30–3.18 (m, 2 H), 1.40–1.24 (m, 9 H); MS (CI) m/e 400 (MH^+), 340.

2-Ethyl 1-Methyl 7-[2-(Diethoxyphosphinyl)ethenyl]-3,4-dihydro-1,2(1H)-isoquinolinedicarboxylate (131). Compound 128 (2.45 g, 9.34 mmol) gave 131 as a pale yellow solid (1.55 g, 39%) by the method described for the preparation of 107: mp 98–100 °C; IR (KBr) 1738, 1692 cm^{-1} ; ^1H NMR (250 MHz, CDCl_3) δ 7.61 (s, 1 H), 7.53 (dd, 1 H, $J = 22.5$, 5.0), 7.39 (d, 1 H, $J = 6.4$), 7.19 (d, 1 H, $J = 7.8$), 6.25 (t, 1 H, $J = 17.4$), 5.60 (d, 1 H, $J = 24.5$), 4.26–4.08 (m, 6 H), 3.84–3.79 (m, 2 H), 3.74 (s, 3 H), 2.99–2.91 (m, 2 H), 1.39–1.24 (m, 9 H); MS (CI) m/e 426 (MH^+), 366 ($\text{MH}^+ - 60$). Anal. ($\text{C}_{20}\text{H}_{28}\text{NO}_7\text{P}$) C, H, N.

2-Ethyl 1-Methyl 7-[2-(Diethoxyphosphinyl)ethyl]-3,4-dihydro-1,2(1H)-isoquinolinedicarboxylate (132). Compound 131 (1.46 g, 3.43 mmol) gave 132 as an oil (1.36 g, 93%) by the method described for the preparation of 108: ^1H NMR (250 MHz, CDCl_3) δ 7.31 (s, 1 H), 7.10 (s, 2 H), 5.56 (d, 1 H, $J = 22.6$), 4.27–4.05 (m, 6 H), 3.94–3.64 (m, 2 H), 3.72 (s, 3 H), 2.95–2.79 (m, 4 H), 2.09–1.97 (m, 2 H), 1.44–1.23 (m, 9 H).

(64) Mori, M.; Chiba, K.; Ban, Y. Reactions and Syntheses with Organometallic Compounds. 7. Synthesis of Benzolactams by Palladium-Catalyzed Amidation. *J. Org. Chem.* 1977, 43, 1684–1687.

1,2,3,4-Tetrahydro-5-phosphono-1-isoquinolinecarboxylic Acid (94). A mixture of 129 (1.00 g, 2.50 mmol) in 20 mL of aqueous 6 N HCl was heated at reflux for 72 h. After cooling, the reaction mixture was washed with ether and the aqueous phase was concentrated. The residue was dissolved in 15 mL of H₂O and freeze-dried, and the resulting foamy solid was dried in vacuo (100 °C, over P₂O₅) to give 94 as a tan solid (0.50 g, 67%): ¹H NMR (250 MHz, D₂O) δ 7.87 (m, 1 H), 7.75 (d, 1 H, *J* = 7.9), 7.59–7.41 (m, 1 H), 5.41 (s, 1 H), 3.67–3.43 (m, 2 H), 3.41–3.32 (m, 2 H); MS (FAB) *m/e* 258 (MH⁺). Anal. (C₁₀H₁₂NO₅P·HCl·0.2H₂O) C, H, N, Cl.

1,2,3,4-Tetrahydro-7-phosphono-1-isoquinolinecarboxylic Acid (96). A suspension of 130 (2.63 g, 6.56 mmol) in 30 mL of aqueous 6 N HCl was heated at reflux for 46 h. After decolorizing with activated charcoal, the reaction mixture was filtered and concentrated. The residue was dissolved in H₂O (15 mL) and freeze-dried to give 96 as a white solid (0.93 g, 55%): mp 160–185 °C (with gas evolution); ¹H NMR (250 MHz, D₂O) δ 7.94 (d, 1 H, *J* = 14.0), 7.71 (dd, 1 H, *J* = 12.5, 7.9), 7.40 (dd, 1 H, *J* = 7.9, 3.4), 5.40 (s, 1 H), 3.69–3.60 (m, 2 H), 3.19–3.14 (m, 2 H); MS (FAB) 258 (MH⁺). Anal. (C₁₀H₁₂NO₅P·HCl) C, H, N; Cl: calcd, 12.07; found, 11.60.

1,2,3,4-Tetrahydro-7-(2-phosphonoethyl)-1-isoquinolinecarboxylic Acid (98). A solution of 132 (1.25 g, 2.92 mmol) in 20 mL of aqueous 6 N HCl was heated at reflux for 72 h. The reaction mixture was washed with ether and the aqueous phase was concentrated. The residue was dissolved in 20 mL of H₂O and freeze-dried. Upon exposure to the atmosphere, the product softened to an oil and later solidified to give 98 as a tan solid (0.78 g, 79%): mp 111–114 °C; ¹H NMR (250 MHz, D₂O) δ 7.33 (s, 1 H), 7.19–7.10 (m, 2 H), 5.14 (s, 1 H), 3.54–3.40 (m, 2 H), 2.96 (t, 2 H, *J* = 6.4), 2.82–2.71 (m, 2 H), 2.01–1.87 (m, 2 H); MS (FAB) *m/e* 286 (MH⁺). Anal. (C₁₂H₁₆NO₅P·HCl·1.5H₂O) C, H, N, Cl.

Diethyl [[4-(Cyanomethyl)phenyl]methyl]phosphonate (136). A solution of 134¹¹ (15.0 g, 47 mmol), potassium cyanide (4.6 g, 70 mmol), and sodium iodide (0.5 g, 3.3 mmol) in 50 mL of acetone and 15 mL of H₂O was heated at 50 °C for 48 h, diluted with H₂O, and extracted with CH₂Cl₂. The organic extracts were washed with H₂O, dried (Na₂SO₄), and concentrated to give 136 as a gold liquid (13.0 g, 100%): ¹H NMR (100 MHz, CDCl₃) δ 7.25 (s, 4 H), 4.05–3.85 (m, 4 H), 3.73 (d, 2 H, *J* = 1.7), 3.13 (d, 2 H, *J* = 21.7), 1.29 (t, 6 H, *J* = 7.1).

Diethyl [[3-(Cyanomethyl)phenyl]methyl]phosphonate (135). Compound 133¹¹ (15.0 g, 46.7 mmol) gave 135 as a gold liquid (12.9 g, 100%) by the method described for the preparation of 136: ¹H NMR (100 MHz, CDCl₃) δ 7.20–7.00 (m, 4 H), 4.10–3.70 (m, 4 H), 3.58 (s, 2 H), 3.03 (d, 2 H, *J* = 21.0), 1.12 (t, 6 H, *J* = 7.0).

Diethyl [[4-(2-Aminoethyl)phenyl]methyl]phosphonate (138). A solution of 136 (3.4 g, 12.7 mmol) in a methanol/ammonia solution was hydrogenated over Raney nickel. The resulting solution was filtered and concentrated to give 138 as a pale green oil (3.26 g, 95%): ¹H NMR (100 MHz, CDCl₃) δ 7.20–6.98 (m, 4 H), 4.00–3.75 (m, 4 H), 3.50–2.50 (m, 4 H), 3.00 (d, 2 H, *J* = 22.0), 1.18 (t, 6 H, *J* = 7.1).

Diethyl [[3-(2-Aminoethyl)phenyl]methyl]phosphonate (137). A suspension of sodium borohydride (1.62 g, 42.8 mmol) in 20 mL of THF was treated successively with a mixture of trifluoroacetic acid (3.2 mL, 41.5 mmol) in 5 mL of THF and a solution of 135 (11.21 g, 41.9 mmol) in 20 mL of THF. After stirring at room temperature overnight, the reaction mixture was concentrated, the residue dissolved in CH₂Cl₂, and the solution washed with H₂O. The organic phase was dried (Na₂SO₄) and concentrated to give 137 as a yellow oil (8.93 g, 77%): ¹H NMR (100 MHz, CDCl₃) δ 7.30–6.90 (m, 4 H), 4.10–3.75 (m, 4 H), 3.20–2.60 (m, 6 H), 1.30–1.05 (m, 6 H).

Ethyl [2-[3-[(Diethoxyphosphinyl)methyl]phenyl]ethyl]carbamate (139). A solution of 137 (1.44 g, 5.29 mmol) and triethylamine (0.82 mL, 5.82 mmol) in 10 mL of CH₂Cl₂ was cooled to 0 °C and treated with ethyl chloroformate (0.56 mL, 5.82 mmol). After warming to room temperature and stirring overnight, the reaction mixture was diluted with 50 mL of CH₂Cl₂ and washed with saturated aqueous NaHCO₃ (20 mL). The organic phase was dried (Na₂SO₄) and concentrated, and the residue was purified by chromatography (EtOAc) to give 139 as an oil (1.37 g, 75%): ¹H NMR (200 MHz, CDCl₃) δ 7.31–7.06 (m,

4 H), 4.68 (bs, 1 H), 4.16–3.95 (m, 6 H), 3.48–3.39 (m, 2 H), 3.13 (d, 2 H, *J* = 21.5), 2.80 (t, 2 H, *J* = 6.9), 1.32–1.19 (m, 9 H).

Ethyl [2-[4-[(Diethoxyphosphinyl)methyl]phenyl]ethyl]carbamate (140). Compound 138 (3.2 g, 11.8 mmol) gave 140 as an oil (4.3 g) by the method described for the preparation of 139. This material was used without further purification in the preparation of 142: ¹H NMR (100 MHz, CDCl₃) δ 7.30–7.00 (m, 4 H), 4.30–4.00 (m, 6 H), 3.30–3.10 (m, 4 H), 3.05 (d, 2 H, *J* = 22.0), 1.30–1.10 (m, 9 H).

6-[(Diethoxyphosphinyl)methyl]-3,4-dihydro-1,2(1*H*)-isoquinolinedicarboxylic Acid, 2-Ethyl Ester (141), and 8-[(Diethoxyphosphinyl)methyl]-3,4-dihydro-1,2(1*H*)-isoquinolinedicarboxylic Acid, 2-Ethyl Ester (143). A solution of 139 (0.69 g, 2.01 mmol) and glyoxylic acid monohydrate (0.17 g, 1.84 mmol) in 4 mL of 3:1 acetic acid/sulfuric acid mixture was stirred at room temperature for 44 h. The reaction mixture was poured into H₂O (50 mL) and extracted into EtOAc (3 × 50 mL). The combined organic phases were dried (Na₂SO₄) and concentrated to give a 6:1 mixture of 141 and 143 as a brown oil (0.64 g, 80%). Spectral data for 141: ¹H NMR (300 MHz, CDCl₃) δ 7.45 (d, 1 H, *J* = 7.7), 7.24–7.11 (m, 2 H), 5.57 (d, 1 H, *J* = 20.2), 4.22 (q, 2 H, *J* = 7.3), 4.16–3.99 (m, 4 H), 3.78 (t, 2 H, *J* = 5.7), 3.13 (d, 2 H, *J* = 21.8), 2.93–2.83 (m, 2 H), 1.34–1.18 (m, 9 H).

7-[(Diethoxyphosphinyl)methyl]-3,4-dihydro-1,2(1*H*)-isoquinolinedicarboxylic Acid, 2-Ethyl Ester (142). Compound 140 (4.2 g, 12.2 mmol) gave 142 as an oil (5.4 g) by the method described for the preparation of 141. This material was used without further purification in the preparation of 145.

2-Ethyl 1-Methyl 7-[(Diethoxyphosphinyl)methyl]-3,4-dihydro-1,2(1*H*)-isoquinolinedicarboxylate (145). A solution of 142 (5.4 g, 13.5 mmol) in THF was treated with an ethereal solution of diazomethane until a yellow color persisted. The reaction mixture was concentrated and the residue purified by chromatography (gradient elution, 50–100% EtOAc in heptane) to give 145 as an oil (3.85 g, 69%): IR (film) 1748, 1701 cm⁻¹; ¹H NMR (100 MHz, CDCl₃) δ 7.47–7.03 (m, 3 H), 6.58 (d, 1 H, *J* = 8.3), 4.29–3.73 (m, 8 H), 3.68 (s, 3 H), 3.12 (d, 2 H, *J* = 20.7), 2.98–2.71 (m, 2 H), 1.43–1.09 (m, 9 H).

Diethyl 6-[(Diethoxyphosphinyl)methyl]-3,4-dihydro-1,2(1*H*)-isoquinolinedicarboxylate (144) and Diethyl 8-[(Diethoxyphosphinyl)methyl]-3,4-dihydro-1,2(1*H*)-isoquinolinedicarboxylate (146). A mixture of 141 and 143 (0.59 g, 0.48 mmol) in a 95:5 EtOH/H₂SO₄ mixture (10 mL) was heated at reflux for 24 h, poured into H₂O, and extracted with CH₂Cl₂ (4 × 50 mL). The combined organic extracts were dried (Na₂SO₄) and concentrated, and the residue was purified by chromatography (EtOAc) to give a greater than 95:5 mixture of 144 and 146 as an oil (0.28 g, 44%). Spectral data for 144: IR (film) 1744, 1701 cm⁻¹; ¹H NMR (300 MHz, CDCl₃) δ 7.46–7.42 (m, 1 H), 7.16–7.10 (m, 2 H), 5.53 (d, 1 H, *J* = 28.6), 4.21–3.78 (m, 10 H), 3.11 (d, 2 H, *J* = 21.7), 3.00–2.78 (m, 2 H), 1.32–1.22 (m, 12 H); MS (EI) *m/e* 345 (M⁺ – 73).

1,2,3,4-Tetrahydro-6-(phosphonomethyl)-1-isoquinolinecarboxylic Acid (95). A solution of 144 (0.24 g, 0.56 mmol) in 10 mL of aqueous 6 N HCl was heated at reflux for 32 h. After concentration, the residue was dissolved in H₂O and freeze-dried to give 95 as a solid (0.10 g, 52%): ¹H NMR (200 MHz, DMSO) δ 9.35 (bs, 1 H), 7.37 (d, 1 H, *J* = 7.9), 7.15 (d, 1 H, *J* = 8.1), 7.11 (s, 1 H), 5.26 (s, 1 H), 3.50–3.30 (m, 2 H), 2.95 (s, 3 H), 2.88 (s, 1 H); MS (FAB) *m/e* 272 (MH⁺). Anal. (C₁₁H₁₄NO₅P·1.3HCl·1.3H₂O) C, N, Cl; H: calcd, 5.28; found, 4.55.

1,2,3,4-Tetrahydro-7-(phosphonomethyl)-1-isoquinolinecarboxylic Acid (97). Compound 145 (3.6 g, 8.7 mmol) gave 97 as a tan solid (2.6 g, 97%) by the method described for the preparation of 95: ¹H NMR (100 MHz, D₂O) δ 7.48 (s, 1 H), 7.27 (s, 2 H), 5.29 (s, 1 H), 3.73–3.47 (m, 2 H), 3.33–1.98 (m, 4 H); MS (FAB) *m/e* 272 (MH⁺). Anal. (C₁₁H₁₄NO₅P·HCl) C, H, N; calcd, 4.55; found, 4.05.

Ethyl 4-Bromo-*N*-acetylphenylalaninate (147). A solution of 150 (5.00 g, 12.9 mmol) and potassium trimethylsilanolate (1.74 g, 13.6 mmol) in 50 mL of THF was stirred at room temperature for 18 h, acidified with aqueous 1 N HCl (20 mL), and extracted with EtOAc. The combined organic extracts were concentrated, and the residue was dissolved in 100 mL of toluene and heated at reflux for 5 h. After concentration, the residue was purified by chromatography (3:1 heptane/ethyl acetate) to give 147 as an

oil (1.42 g, 35%) and recovered starting material (2.34 g): $^1\text{H NMR}$ (250 MHz, CDCl_3) δ 7.41 (d, 2 H, $J = 8.4$), 6.97 (d, 2 H, $J = 8.4$), 6.00 (d, 1 H, $J = 7.0$), 4.88–4.80 (m, 1 H), 4.18 (q, 2 H, $J = 7.3$), 3.11–3.06 (m, 2 H), 1.99 (s, 3 H), 1.25 (t, 3 H, $J = 7.1$).

Ethyl 3-[(Diethylphosphono)methyl]-*N*-acetylphenylalaninate (148). A solution of diethyl (acetylamino)[[3-[(diethoxyphosphinylmethyl)phenyl]methyl]propanedioate¹¹ (0.43 g, 0.96 mmol) in 4 mL of THF gave 148 as an oil (0.14 g, 38%) by the method described for the preparation of 147: $^1\text{H NMR}$ (250 MHz, CDCl_3) δ 7.27–7.00 (m, 4 H), 6.18 (d, 1 H, $J = 7.3$), 4.90–4.82 (m, 1 H), 4.14 (q, 2 H, $J = 7.1$), 4.04–3.90 (m, 4 H), 3.15–3.02 (m, 4 H), 2.02 (s, 3 H), 1.28–1.21 (m, 9 H).

Diethyl (Acetylamino)[(2-bromophenyl)methyl]propanedioate (149). A solution of 0.5 M sodium ethoxide (800 mL) was treated with diethyl acetamidomalonate (87.2 g, 0.40 mol). After stirring at room temperature overnight, a solution of 2-bromobenzyl bromide (100 g, 0.40 mol) in 100 mL of EtOH was added dropwise, and the resulting solution was stirred at room temperature for 48 h. The reaction mixture was concentrated, and the residue was treated with EtOAc (200 mL) and H_2O (200 mL). The aqueous phase was extracted with additional EtOAc (3 \times 200 mL), and the combined organic extracts were dried (MgSO_4) and concentrated, and the residue was recrystallized from 1:1 *i*-Pr₂O/heptane (900 mL) to give 149 as a white solid (114 g, 74%). Anal. ($\text{C}_{16}\text{H}_{20}\text{BrNO}_5$) C, H, N.

Diethyl (Acetylamino)[(4-bromophenyl)methyl]propanedioate (150). 4-Bromobenzyl bromide (50.0 g, 0.20 mmol) gave 150 as a white solid (41.3 g, 53%) by the method described for the preparation of 149.

2-Bromophenylalanine Hydrochloride (151). A suspension of 149 (110 g, 0.285 mol) in 1 L of aqueous 6 N HCl was heated at reflux for 18 h. The resulting white solid was collected and dried *in vacuo* to give 151 (71.5 g, 89%). Anal. ($\text{C}_9\text{H}_{10}\text{BrNO}_2\text{HCl}$) C, H, N, Cl.

4-Bromophenylalanine Hydrochloride (152). Compound 150 (20.0 g, 51.8 mmol) gave 152 as a white solid (17.3 g) by the method described for the preparation of 151. This material was used without further purification in the preparation of 155.

2-Bromo-*N*-(methoxycarbonyl)phenylalanine (153). A solution of 151 (35.0 g, 0.125 mol) in 190 mL of aqueous 1 N NaOH was treated dropwise with methyl chloroformate (18 mL, 0.232 mol). Additional aqueous 1 N NaOH was added as necessary to maintain a pH of approximately 10. The resulting solution was extracted with ether (2 \times 200 mL) and the aqueous phase was acidified (pH = 2) with concentrated HCl. The aqueous phase was extracted with CH_2Cl_2 (3 \times 300 mL), and the combined organic extracts were dried (Na_2SO_4) and concentrated to give 153 as a white solid (26.6 g, 71%).

4-Bromo-*N*-(methoxycarbonyl)phenylalanine (155). Compound 152 (17.0 g) gave 155 by the method described for the preparation of 153.

Methyl 2-Bromo-*N*-(methoxycarbonyl)phenylalaninate (154). A solution of 153 (26.6 g, 88.0 mmol) in 100 mL of THF was treated with an ethereal solution of diazomethane until a persistent yellow color developed. The resulting solution was concentrated to give 154 as an oil (26.6 g, 96%): $^1\text{H NMR}$ (250 MHz, CDCl_3) δ 7.55 (d, 1 H, $J = 7.9$), 7.29–7.08 (m, 3 H), 5.30 (bs, 1 H), 4.74–4.65 (m, 1 H), 3.72 (s, 3 H), 3.63 (s, 3 H), 3.33–3.10 (m, 2 H).

Methyl 4-Bromo-*N*-(methoxycarbonyl)phenylalaninate (156). Compound 155 gave 156 as an oil (18.3 g, 95% overall from 152) by the method described for the preparation of 154: $^1\text{H NMR}$ (250 MHz, CDCl_3) δ 7.41 (d, 2 H, $J = 7.4$), 6.99 (d, 2 H, $J = 7.4$), 5.20 (bs, 1 H), 4.67–4.59 (m, 1 H), 3.72 (s, 3 H), 3.67 (s, 3 H), 3.14–2.98 (m, 2 H).

Dimethyl 5-Bromo-3,4-dihydro-2,3(1*H*)-isoquinolinedicarboxylate (157). A solution of 154 (14.7 g, 46.5 mmol) in a 3:1 glacial acetic acid/concentrated sulfuric acid mixture (60 mL) was treated with paraformaldehyde (1.47 g, 49 mmol). After stirring at room temperature for 24 h, the reaction mixture was poured into H_2O and extracted with ethyl acetate (4 \times 50 mL). The combined organic extracts were washed with saturated aqueous NaHCO_3 solution, dried (MgSO_4), and concentrated, and the residue was purified by chromatography (3:1 heptane/EtOAc) to give 157 as an oil (5.15 g, 33%): IR (film) 1745, 1708 cm^{-1} ; $^1\text{H NMR}$ (250 MHz, CDCl_3) δ 7.46–7.42 (m, 1 H), 7.09–7.05 (m, 2 H),

5.22–5.20 (m, 0.6 H), 5.02–5.00 (m, 0.4 H), 4.85–4.49 (m, 2 H), 3.78 (d, 3 H, $J = 10.9$), 3.66 (s, 3 H), 3.59–3.48 (m, 1 H), 3.10–3.00 (m, 1 H); MS (EI) 330, 328 ($\text{M}^+ + 1$).

Dimethyl 7-Bromo-3,4-dihydro-2,3(1*H*)-isoquinolinedicarboxylate (158). Compound 156 (9.00 g, 28.4 mmol) gave 158 as a white solid (3.23 g, 35%) by the method described for the preparation of 157: mp 101–103 °C; IR (KBr) 1745, 1711 cm^{-1} ; $^1\text{H NMR}$ (250 MHz, CDCl_3) δ 7.31–7.25 (m, 2 H), 7.02 (d, 1 H, $J = 8.1$), 5.20–5.16 (m, 0.6 H), 4.98–4.96 (m, 0.4 H), 4.77–4.47 (m, 2 H), 3.78 (d, 3 H, $J = 12.7$), 3.63 (s, 3 H), 3.33–3.04 (m, 2 H); MS (EI) m/e 329, 327 (M^+). Anal. ($\text{C}_{13}\text{H}_{14}\text{BrNO}_4$) C, H, N, Br.

Dimethyl 5-(Diethylphosphinyl)-3,4-dihydro-2,3(1*H*)-isoquinolinedicarboxylate (159). A solution of 157 (2.39 g, 7.28 mmol), diethyl phosphite (1.11 g, 8.01 mmol), and tetrakis(triphenylphosphine)palladium(0) (0.27 g, 0.23 mmol) in 20 mL of toluene containing 1.15 mL of triethylamine was heated at reflux for 48 h. The reaction mixture was cooled to room temperature and washed with a saturated aqueous NaHCO_3 solution. The aqueous phase was extracted with EtOAc, and the combined organic extracts were dried (MgSO_4) and concentrated. The residue was purified by chromatography (EtOAc) to give 159 as an oil (1.54 g, 55%): IR (film) 1745, 1710 cm^{-1} ; $^1\text{H NMR}$ (250 MHz, CDCl_3) δ 7.88–7.80 (m, 1 H), 7.71–7.63 (m, 1 H), 7.33–7.28 (m, 1 H), 5.14–5.11 (m, 0.6 H), 4.94–4.90 (m, 0.4 H), 4.85–4.55 (m, 2 H), 4.21–4.06 (m, 4 H), 3.84–3.70 (m, 4 H), 3.64 (s, 3 H), 3.38–3.20 (m, 1 H), 1.43–1.27 (m, 6 H); MS (CI) m/e 386 (MH^+).

Dimethyl 7-(Diethylphosphinyl)-3,4-dihydro-2,3(1*H*)-isoquinolinedicarboxylate (160). Compound 158 (2.00 g, 6.09 mmol) gave 160 as an oil (2.03 g, 87%) by the method described for the preparation of 159: IR (film) 1747, 1706 cm^{-1} ; $^1\text{H NMR}$ (250 MHz, CDCl_3) δ 7.71–7.47 (m, 3 H), 5.22–5.18 (m, 0.6 H), 5.07–5.00 (m, 0.4 H), 4.90–4.54 (m, 2 H), 4.20–4.02 (m, 4 H), 3.79 (d, 3 H, $J = 12.6$), 3.64 (s, 3 H), 3.29–3.16 (m, 2 H), 1.33 (t, 6 H, $J = 7.1$); MS (CI) m/e 386 (MH^+).

Dimethyl 5-[2-(Diethylphosphinyl)ethenyl]-3,4-dihydro-2,3(1*H*)-isoquinolinedicarboxylate (161). A solution of 157 (4.50 g, 13.7 mmol), diethyl vinylphosphonate (2.54 g, 15.5 mmol), and bis(triphenylphosphine)palladium(II) dichloride (0.39 g, 0.55 mmol) in 35 mL of the dimethylformamide and 7 mL triethylamine was heated at 90 °C for 24 h. The reaction mixture was concentrated and the residue purified by chromatography (EtOAc) to give 161 as a brown oil (2.26 g, 40%): $^1\text{H NMR}$ (250 MHz, CDCl_3) δ 7.76 (dd, 1 H, $J = 22.3, 17.5$), 7.43 (d, 1 H, $J = 7.4$), 7.23–7.11 (m, 3 H), 6.19 (t, 1 H, $J = 17.5$), 5.20–5.17 (m, 0.6 H), 5.02–4.84 (m, 0.4 H), 4.85–4.50 (m, 2 H), 4.21–4.07 (m, 4 H), 3.78 (d, 3 H, $J = 12.0$), 3.63 (s, 3 H), 3.49–3.38 (m, 1 H), 3.18–3.04 (m, 1 H), 1.37 (t, 6 H, $J = 7.1$).

Dimethyl 7-[2-(Diethylphosphinyl)ethenyl]-3,4-dihydro-2,3(1*H*)-isoquinolinedicarboxylate (163). Compound 158 (2.45 g, 7.47 mmol) gave 163 as a yellow oil (1.20 g, 39%) by the method described for the preparation of 161: $^1\text{H NMR}$ (250 MHz, CDCl_3) δ 7.68–7.15 (m, 4 H), 6.38–6.11 (m, 1 H), 5.21–5.19 (m, 0.6 H), 5.05–4.96 (m, 0.4 H), 4.85–4.44 (m, 2 H), 4.18–4.04 (m, 4 H), 3.79 (d, 3 H, $J = 13.9$), 3.62 (s, 3 H), 3.17–3.13 (m, 2 H), 1.38–1.23 (m, 6 H).

Dimethyl 5-[2-(Diethylphosphinyl)ethyl]-3,4-dihydro-2,3(1*H*)-isoquinolinedicarboxylate (162). A solution of 161 (2.26 g, 5.49 mmol) in 100 mL of MeOH was hydrogenated at 52 psi over 10% Pd/C. The reaction mixture was filtered and concentrated, and the residue was purified by chromatography (EtOAc) to give 162 as an oil (1.44 g, 63%): IR (film) 1742, 1709 cm^{-1} ; $^1\text{H NMR}$ (250 MHz, CDCl_3) δ 7.18–7.05 (m, 3 H), 5.21–5.18 (m, 0.6 H), 5.02–4.97 (m, 0.4 H), 4.79–4.52 (m, 2 H), 4.15–4.06 (m, 4 H), 3.84 (d, 3 H, $J = 13.0$), 3.62 (s, 3 H), 3.41–3.31 (m, 1 H), 3.04–2.85 (m, 3 H), 2.02–1.79 (m, 2 H), 1.37–1.30 (m, 6 H); MS (FAB) m/e 412 ($\text{MH}^+ - 2$).

Dimethyl 7-[2-(Diethylphosphinyl)ethyl]-3,4-dihydro-2,3(1*H*)-isoquinolinedicarboxylate (164). Compound 163 (1.24 g, 3.01 mmol) gave 164 as an oil (0.62 g, 50%) by the method described for the preparation of 162: IR (film) 1742, 1709 cm^{-1} ; $^1\text{H NMR}$ (250 MHz, CDCl_3) δ 7.09–6.94 (m, 3 H), 5.19–5.13 (m, 0.6 H), 4.98–4.93 (m, 0.4 H), 4.81–4.43 (m, 2 H), 4.15–4.03 (m, 4 H), 3.78 (d, 3 H, $J = 13.9$), 3.62 (s, 3 H), 3.24–3.17 (m, 2 H), 2.92–2.82 (m, 2 H), 2.09–1.95 (m, 2 H), 1.32 (t, 6 H, $J = 7.4$); MS (FAB) m/e 412 ($\text{MH}^+ - 2$).

1,2,3,4-Tetrahydro-5-phosphono-3-isoquinolinecarboxylic

Acid (87). A solution of 159 (1.56 g, 4.05 mmol) in 30 mL of 6 N HCl was heated at reflux for 24 h. After concentration, the residue was suspended in H₂O and filtered, and the white solid was dried in vacuo (100 °C over P₂O₅) to give 87 (0.59 g, 56%): mp 192–195 °C; ¹H NMR (250 MHz, D₂O/NaOD) δ 7.65–7.27 (m, 1 H), 7.23–7.12 (m, 2 H), 4.04 (s, 2 H), 3.63 (dd, 1 H, *J* = 16.8, 4.2), 3.45 (dd, 1 H, *J* = 11.2, 4.2), 2.94 (dd, 1 H, *J* = 16.8, 11.6); MS (FAB) *m/e* 258 (MH⁺). Anal. (C₁₀H₁₂NO₅P·0.07HCl) C, H, N, Cl.

1,2,3,4-Tetrahydro-7-phosphono-3-isoquinolinecarboxylic Acid (91). A solution of 160 (2.01 g, 5.21 mmol) in 20 mL of 6 N HCl was heated at reflux for 48 h, cooled to room temperature, and washed with ether. The aqueous phase was concentrated, and the residue dissolved in 20 mL of H₂O and freeze-dried to give 91 as a white solid (0.92 g, 61%): ¹H NMR (250 MHz, D₂O) δ 7.73–7.61 (m, 2 H), 7.45 (dd, 1 H, *J* = 7.9, 7.5), 4.57–4.46 (m, 3 H), 3.57 (dd, 1 H, *J* = 17.7, 5.4), 3.33 (dd, 1 H, *J* = 17.7, 11.0); MS (FAB) *m/e* 258 (MH⁺). Anal. (C₁₀H₁₂NO₅P·0.9HCl) C, H, N, Cl.

1,2,3,4-Tetrahydro-5-(2-phosphonoethyl)-3-isoquinolinecarboxylic Acid (89). A solution of 162 (1.26 g, 3.05 mmol) in 20 mL of 6 N HCl was heated at reflux for 24 h. The reaction mixture was concentrated, and the residue was dissolved in 20 mL of H₂O and freeze-dried. The resulting solid was purified by ion exchange chromatography (Dowex 50 × 4–400 ion exchange resin), eluting with a 2 M NH₄OH solution. The eluant was freeze-dried and then dried under vacuum (100 °C, P₂O₅) to give 89 as a tan solid (0.44 g, 45%): mp 215–240 °C (decomposed with gas evolution); ¹H NMR (250 MHz, D₂O) δ 7.37–7.24 (m, 2 H), 7.13–7.09 (m, 1 H), 4.41 (s, 2 H), 4.03 (dd, 1 H, *J* = 11.0, 4.9), 3.43 (dd, 1 H, *J* = 17.1, 4.9), 3.10 (dd, 1 H, *J* = 17.1, 11.0), 2.89–2.79 (m, 2 H), 1.77–1.61 (m, 2 H); MS (FAB) *m/e* 286 (MH⁺). Anal. (C₁₂H₁₄NO₅P·1.5NH₃·0.7H₂O) C, N, H; calcd, 6.83; found, 6.30.

1,2,3,4-Tetrahydro-7-(2-phosphonoethyl)-3-isoquinolinecarboxylic Acid (93). Compound 164 (0.62 g, 1.50 mmol) gave 93 as a white solid (0.18 g, 63%) by the method described for the preparation of 87: ¹H NMR (250 MHz, D₂O) δ 7.16 (s, 2 H), 7.09 (s, 1 H), 3.99 (ABq, 2 H, *J*_{AB} = 16.2, Δ*v*_{AB} = 16.5), 3.45 (dd, 1 H, *J* = 10.8, 4.4), 3.05 (dd, 1 H, *J* = 16.5, 4.3), 2.86–2.72 (m, 3 H), 1.73–1.60 (m, 2 H). Anal. (C₁₂H₁₆NO₅P·0.14HCl) H, N, Cl; C: calcd, 49.64; found, 50.27.

Diethyl [(2-Bromophenyl)methyl] [(ethoxycarbonyl)amino]propanedioate (169). An 0.2 M solution of NaOEt (500 mL) was treated with diethyl *N*-carbethoxymalonate⁶⁵ (25 g, 100 mmol). The resulting solution was stirred at room temperature for 1 h and treated dropwise with a solution of 2-bromobenzyl bromide (165) (25.0 g, 100 mmol) in 100 mL of EtOH. The reaction mixture was stirred at room temperature for 24 h and concentrated, and the residue was partitioned between CH₂Cl₂ (300 mL) and H₂O (200 mL). The organic phase was separated and the aqueous phase was extracted with additional CH₂Cl₂ (2 × 150 mL). The combined organic extracts were dried (MgSO₄), filtered, and concentrated. The residue was purified by chromatography (3:1 heptane/EtOAc) to give 169 as an oil (30.32 g, 73%).

Diethyl [[2-[(Diethoxyphosphinyl)methyl]phenyl]methyl] [(ethoxycarbonyl)amino]propanedioate (170). NaOEt (19.1 mmol) in 50 mL of EtOH was treated with diethyl *N*-carbethoxymalonate⁶⁵ (4.62 g, 18.7 mmol) in one portion and stirred at room temperature for 1 h. A solution of 166¹¹ (6.00 g, 18.7 mmol) in 5 mL of ethanol was added dropwise, and the resulting solution was stirred for 24 h at room temperature. The reaction mixture was concentrated and the residue partitioned between EtOAc (100 mL) and H₂O (100 mL). The organic layer was separated and the aqueous layer extracted with additional EtOAc (3 × 100 mL). The combined organic extracts were dried (MgSO₄) and concentrated, and the residue was purified by chromatography (EtOAc) to give 170 as an oil (6.91 g, 76%): ¹H NMR (250 MHz, CDCl₃) δ 7.40–6.99 (m, 4 H), 5.90 (bs, 1 H), 4.40–3.99 (m, 10 H), 3.73 (s, 2 H), 3.17 (d, 2 H, *J* = 21.2), 1.30–1.19 (m, 15 H).

Diethyl [[3-[(Diethoxyphosphinyl)methyl]phenyl]methyl] [(ethoxycarbonyl)amino]propanedioate (171). Compound 167¹¹ (2.46 g, 7.66 mmol) gave 171 as an oil (2.33 g,

63%) by the method described for the preparation of 170: ¹H NMR (250 MHz, CDCl₃) δ 7.24–7.20 (m, 2 H), 6.96–6.92 (m, 2 H), 5.86 (bs, 1 H), 4.36–3.88 (m, 10 H), 3.60 (s, 2 H), 3.09 (d, 2 H, *J* = 22.6), 1.37–1.21 (m, 15 H).

Diethyl [[4-[(Diethoxyphosphinyl)methyl]phenyl]methyl] [(ethoxycarbonyl)amino]propanedioate (172). Compound 168 (3.00 g, 9.34 mmol) gave 172 as an oil (3.32 g, 73%) by the method described for the preparation of 170: ¹H NMR (250 MHz, CDCl₃) δ 7.21 (dd, 2 H, *J* = 13.9, 7.8), 6.99 (d, 2 H, *J* = 7.8), 5.84 (bs, 1 H), 4.48–3.97 (m, 10 H), 3.60 (s, 2 H), 3.11 (d, 2 H, *J* = 21.6), 1.36–1.19 (m, 15 H).

Triethyl 5-Bromo-1,4-dihydro-2,3,3-isoquinolinetricarboxylate (173). Compound 169 (9.78 g, 23.4 mmol) gave 173 as an oil (5.79 g, 57%), after purification of the crude reaction mixture by chromatography (1:1 heptane/EtOAc), by the method described for the preparation of 157: IR (film) 1750, 1710 cm⁻¹; ¹H NMR (250 MHz, CDCl₃) δ 7.48–7.44 (m, 1 H), 7.19–7.05 (m, 2 H), 4.67 (d, 2 H, *J* = 6.9), 4.25–4.14 (m, 6 H), 3.61 (s, 2 H), 1.34 (t, 3 H, *J* = 7.1), 1.22 (t, 6 H, *J* = 7.2); MS (EI) *m/e* 429, 427 (M⁺).

Triethyl 5-[(Diethoxyphosphinyl)methyl]-1,4-dihydro-2,3,3-isoquinolinetricarboxylate (174). Compound 170 (4.43 g, 9.09 mmol) gave 174 as an oil (3.97 g, 87%) by the method described for the preparation of 157: IR (film) 1751, 1709 cm⁻¹; ¹H NMR (250 MHz, CDCl₃) δ 7.28–7.06 (m, 3 H), 4.67 (d, 2 H, *J* = 10.0), 4.22–3.96 (m, 10 H), 3.47 (s, 2 H), 3.23 (d, 2 H, *J* = 21.6), 1.43–1.16 (m, 15 H); MS (CI) *m/e* 500 (MH⁺).

Triethyl 6-[(Diethoxyphosphinyl)methyl]-1,4-dihydro-2,3,3-isoquinolinetricarboxylate (175). Compound 171 (3.27 g, 6.74 mmol) gave 175 as an oil (2.87 g, 85%) by the method described for the preparation of 157: IR (film) 1753, 1708 cm⁻¹; ¹H NMR (250 MHz, CDCl₃) δ 7.15–7.09 (m, 3 H), 4.66 (d, 2 H, *J* = 6.6), 4.24–3.94 (m, 10 H), 3.40 (d, 2 H, *J* = 8.8), 3.11 (d, 2 H, *J* = 21.6), 1.36–1.16 (m, 15 H); MS (FAB) 500 (MH⁺).

Triethyl 7-[(Diethoxyphosphinyl)methyl]-1,4-dihydro-2,3,3-isoquinolinetricarboxylate (176). Compound 172 (2.66 g, 4.66 mmol) gave 176 as an oil (1.68 g, 72%) by the method described for the preparation of 157: IR (film) 1751, 1711 cm⁻¹; ¹H NMR (250 MHz, CDCl₃) δ 7.20–7.07 (m, 3 H), 4.67 (d, 2 H, *J* = 7.2), 4.28–3.94 (m, 10 H), 3.40 (d, 2 H, *J* = 8.0), 3.10 (d, 2 H, *J* = 21.6), 1.39–1.15 (m, 15 H); MS (FAB) *m/e* 498 (MH⁺ - 2).

Triethyl 1,4-Dihydro-5-(3-ethoxy-3-oxo-1-propenyl)-2,3,3-isoquinolinetricarboxylate (177). A solution of 173 (2.63 g, 6.14 mmol), ethyl acrylate (0.73 mL, 6.75 mmol), triethylamine (0.68 g, 6.75 mmol), and bis(triphenylphosphine)palladium(II) dichloride (0.20 g, 0.28 mmol) in 50 mL of toluene was heated at reflux for 72 h. The reaction mixture was cooled to room temperature and washed with saturated aqueous NaHCO₃ solution (20 mL). The aqueous phase was extracted with toluene (3 × 30 mL), and the combined organic extracts were dried (MgSO₄), filtered, and concentrated. Purification of the residue by chromatography (3:1 heptane/ethyl acetate) gave 177 as a yellow solid (1.33 g, 48%): ¹H NMR (250 MHz, CDCl₃) δ 7.99 (d, 1 H, *J* = 16.0), 7.48 (d, 1 H, *J* = 7.4), 7.26–7.19 (m, 2 H), 6.37 (d, 1 H, *J* = 15.8), 4.69 (d, 2 H, *J* = 8.1), 4.33–4.12 (m, 8 H), 3.57 (s, 2 H), 1.35 (t, 3 H, *J* = 7.4), 1.18 (t, 9 H, *J* = 7.1).

Triethyl 1,4-Dihydro-5-(3-ethoxy-3-oxopropyl)-2,3,3-isoquinolinetricarboxylate (178). Compound 177 (1.98 g, 4.42 mmol) gave 178 as a yellow oil (1.52 g, 76%) by the method described for the preparation of 162: IR (film) 1756, 1711 cm⁻¹; ¹H NMR (250 MHz, CDCl₃) δ 7.22–7.00 (m, 3 H), 4.66 (d, 2 H, *J* = 7.5), 4.42–4.10 (m, 8 H), 3.44 (s, 2 H), 3.01–2.95 (m, 2 H), 2.58–2.48 (m, 2 H), 1.44–1.28 (m, 12 H); MS (CI) *m/e* 450 (MH⁺).

1,2,3,4-Tetrahydro-5-(phosphonomethyl)-3-isoquinolinecarboxylic Acid (88). Compound 174 (2.00 g, 4.02 mmol) gave 88 as a white solid (1.06 g, 84%) by the method described for the preparation of 96: mp 160–170 °C; ¹H NMR (250 MHz, D₂O) δ 7.32–7.27 (m, 2 H), 7.23–7.17 (m, 1 H), 4.48 (s, 2 H), 4.38 (dd, 1 H, *J* = 11.6, 5.5), 3.61 (dd, 1 H, *J* = 17.7, 5.5), 3.22 (d, 2 H, *J* = 21.4), 3.27–3.18 (m, 1 H); MS (FAB) *m/e* 272 (MH⁺). Anal. (C₁₁H₁₄NO₅P·1.1HCl·0.2H₂O) C, H, N, Cl.

1,2,3,4-Tetrahydro-6-(phosphonomethyl)-3-isoquinolinecarboxylic Acid (90). Compound 175 (2.83 g, 5.67 mmol) gave 90 as a tan solid (1.26 g, 71%) by the method described for the preparation of 96: ¹H NMR (250 MHz, D₂O) δ 7.23 (s, 3 H), 4.47–4.35 (m, 3 H), 3.47 (dd, 1 H, *J* = 17.4, 5.4), 3.30–3.21 (m,

(65) Frankel, M.; Harnik, M.; Levin, Y.; Knobler, Y. Synthesis of Polyaminomalonic Acid. *J. Am. Chem. Soc.* 1953, 75, 78–79.

1 H), 3.17 (d, 2 H, $J = 21.2$); MS (FAB) m/e 272 (MH⁺). Anal. (C₁₁H₁₄NO₅P·HCl) C, H, N, Cl: calcd, 11.52; found, 10.75.

1,2,3,4-Tetrahydro-7-(phosphonomethyl)-3-isoquinoline-carboxylic Acid (92). Compound 176 (1.59 g, 3.18 mmol) gave 92 as a tan solid (0.66 g, 69%) by the method described for the preparation of 96: ¹H NMR (250 MHz, D₂O) δ 7.27 (s, 2 H), 7.18 (s, 1 H), 4.56–4.41 (m, 3 H), 3.53–3.17 (m, 2 H), 3.21 (d, 2 H, $J = 21.4$); MS (FAB) m/e 272 (MH⁺). Anal. (C₁₁H₁₄NO₅P·0.75HCl·0.35H₂O) C, N, Cl, H: calcd 5.11; found, 4.69.

3-Carboxy-1,2,3,4-tetrahydro-5-isoquinolinepropanoic Acid (99). A solution of 178 (1.50 g, 3.34 mmol) gave 99 as a tan solid (0.43 g, 52%) by the method described for the preparation of 96: mp 302–305 °C; ¹H NMR (250 MHz, DMSO) δ 14.20 (bs, 3 H), 7.25–7.09 (m, 3 H), 4.43–4.34 (m, 3 H), 3.32 (dd, 1 H, $J = 17.0$, 5.2), 3.01 (dd, 1 H, $J = 17.0$, 11.4), 2.82 (t, 2 H, $J = 7.4$), 2.52 (t, 2 H, $J = 7.4$); MS (CI) m/e 250 (MH⁺). Anal. (C₁₃H₁₆NO₄·0.2HCl) C, H, N, Cl.

Biology. Displacement of [³H]-3-(2-Carboxypiperazin-4-yl)propylphosphonic Acid (CPP; 1) from NMDA Receptors in Rat Brain Crude Synaptic Membranes. Binding assays with [³H]CPP were carried as previously described.¹¹ Unless otherwise noted, results are an average of six determinations.

Molecular Modeling. Definition of PO₃H₂-Receptor Interaction Geometry. (i) Cambridge Structural Database Search. Using the CAMBRIDGE command within SYBYL, version 3.4, the Cambridge Structural Database was searched using the template PO₃. Of the 82 hits, 32 remained after removing entries with no coordinates (20), those with covalent attachments to the oxygens, and those with PO...OP interactions (30). Examples from the latter category were removed under the assumption that the receptor site being modeled did not contain any interactions of this type. The 32 hits provided 49 examples of PO...X interactions (X = O, N atoms) (Table VII), resulting in an average bond length (d) and valence angle (θ) of 2.73 ± 0.19 Å and $122 \pm 11^\circ$, respectively. Interestingly, only 2 of the 30 interactions contained bifurcated hydrogen bonds; all others contained linear hydrogen bonds off of one of the PO₃H₂ oxygen atoms.

(ii) Brookhaven Protein Data Bank Search. The July, 1987 release was searched for the strings "HETATM" and "P" on the same record. If found, the entry was checked to insure it contained a ligand with a PO₃ moiety. Entries with resolutions ≤ 3.0 Å were then read into SYBYL, and distances and angles between each PO₃ oxygen atom and neighboring heavy atoms in the proteins were measured and recorded. A total of 122 entries resulted, which are summarized in Table VIII. After the entries with improper geometries for strong hydrogen bond formation (O...X distance < 2.5 Å; P–O–X valence angle $< 90^\circ$) were removed, 82 remained, giving a mean O...X bond length of 2.80 ± 0.27 Å and P–O–X valence angle of $128 \pm 19^\circ$. None of the remaining interactions involved bifurcated hydrogen bonds. A listing of the 122 individual distances and valence angle values, together with a frequency distribution analysis on the data using PROC FREQ within SAS,⁶⁶ is included as supplementary material.

The results of the Cambridge and Brookhaven database searches were combined to give average O...X distance and P–O–X

valence angles of 2.8 ± 0.2 Å and $125 \pm 15^\circ$, respectively.

Conformational Searches. In general, all rotatable bonds within the PO₃H₂-containing side chains were scanned from 0 to 359° in 30° increments. In addition, the second phosphonic acid hydroxyl was rotated from 0 to 180° in 30° increments to insure that conformations were not being rejected due to adverse steric or electrostatic interactions from this moiety. Other SEARCH options employed included general, 1–4, and hydrogen-bonding van der Waals factors of 0.8, 0.8, and 0.65, respectively, and an energy cutoff of ≤ 10 kcal/mol above the minimum for acceptance of the conformer. For the energy calculations, CNDO/2 (density matrix-derived) point charges were included, and a PO...X (X = the hypothetical receptor [sp³ nitrogen] atom) default distance and O...X stretching constant of 2.8 Å and 600 kcal/mol were specified. Although the energies obtained have little meaning in an absolute sense because the molecules contained an arbitrary receptor atom, we felt the *relative* differences between energies for multiple conformations of the same structure could be used to select allowed conformations.

To record allowed positions of the hypothetical receptor atom relative to the invariant amino acid moiety within antagonists, three distances were defined (Figure 8). These distances were recorded in a three-dimensional distance map (termed an orientation map in version 3.5 of the SYBYL software), each dimension of which extended from 2 to 12 Å. A grid size of 0.3 Å was used. After intersecting allowed distances among the initial set of active antagonists (Table II, 1, 2, and 19–22) and subtracting distances corresponding to the inactive congeners 23 and 24, a set of 17 distances resulted. To visualize the conformations that gave rise to these distances, an additional search was run on 2 using the 17 distances as a constraint and recording the O...X bond positions in a coordinate map (termed a vector map in version 3.5 of the SYBYL software) (see Figure 9).

Acknowledgment. We wish to thank Laura J. Brahce and Linda L. Coughenour from the Department of Neuroscience for conducting the receptor binding assays, Gary McClusky and staff for the analytical and spectral determinations, and Norm Colbry and Don Johnson for the hydrogenation reactions.

Supplementary Material Available: Coordinates of the fit conformations of CPP (1), NMDA (6), and 1,2,3,4-tetrahydro-5-(2-phosphonoethyl)-3-isoquinolinecarboxylic acid (89), in SYBYL.MOL2 file format; fitting energies, similar to those given in Table I for the agonists, for all competitive antagonists; individual observations from the search of the Brookhaven Protein Databank, together with a statistical (frequency) analysis of the data, run using the SAS⁶⁶ software (22 pages). Ordering information can be found on any current masthead page.

(66) Version 5.18 of the SAS software (SAS Institute, Inc., Cary, NC) was used for the statistical analyses.